Energy Conversion and Management 269 (2022) 116166

Contents lists available at ScienceDirect

Energy Conversion and Management

journal homepage: www.elsevier.com/locate/enconman

The roadmap towards the efficiency limit for supercritical carbon dioxide coal fired power plant

Zhaofu Wang [a], Haonan Zheng [a], Jinliang Xu [a,b,*], Mingjia Li [c], Enhui Sun [a,b], Yuandong Guo [a], Chao Liu [a], Guanglin Liu [a,b]

[a] Beijing Key Laboratory of Multiphase Flow and Heat Transfer for Low Grade Energy Utilization, North China Electric Power University, Beijing 102206, China
[b] Key Laboratory of Power Station Energy Transfer Conversion and System (North China Electric Power University), Ministry of Education, Beijing 102206, China
[c] Key Laboratory of Thermo-Fluid Science and Engineering of Ministry of Education, School of Energy and Power Engineering, Xi'an Jiaotong University, Xi'an, Shaanxi, 710049, China

ARTICLE INFO

Keywords:
sCO_2 cycle
Efficiency limit
Coal-fired power plant
Overlap energy utilization
Module boiler design

ABSTRACT

The Chinese Government has issued a series of documents to explain China's control over the carbon dioxide (CO_2) emission. One of the major tasks is to develop higher efficiency coal fired power plant, compared with current running power plant. In this paper, we aim to explore the roadmap to reach the efficiency limit for coal fired power plant using supercritical carbon dioxide cycle (sCO_2 cycle). Referenced to Carnot cycle, the proposed roadmap is to increase the cycle efficiency by elevating average heat absorption temperature ($T_{ave,h}$) and lowering average heat release temperature ($T_{ave,l}$). In contrast to recompression cycle (RC), tri-compression cycle (TC) is introduced. Due to the increased $T_{ave,h}$, TC achieves the second largest contribution for efficiency increment, followed by the reheating technique. Then, TC, double reheating (DRH) and intercooling (IC) are integrated as TC + DRH + IC in the power plant. To completely absorb flue gas energy over entire temperature range of (1500 ~ 120) °C. A top cycle and a bottom cycle are connected for cascade utilization of flue gas energy. Overlap energy utilization is further utilized to fill the efficiency gap between top and bottom cycles. The proposed cycle also integrates the module boiler design to suppress the pressure drop penalty, and the flue gas recirculation to keep the heater surface temperature in an accepted level. A numerical model is developed for the comprehensive sCO_2 cycle. At the main vapor parameters of 35 MPa/630 °C, the sCO_2 coal fired power plant reaches the net power generation efficiency of 51.03%, which is higher than 48.12% for a supercritical water-steam power plant at the same capacity. Such efficiency improvement saves 175.2 kilotons of coal and reduces 396.4 kilotons of CO_2 emission for 1000 MW capacity in a fascial year. Our work provides the guideline for the design and operation of large scale sCO_2 coal fired power plant.

1. Introduction:

Global climate change is the most significant environmental problem in the 21st century [1]. The Chinese government promises to peak carbon dioxide emissions by 2030 and strives to achieve carbon neutralization by 2060 [2]. China's raw coal production and consumption account for approximately 68.6% and 57.7% of the primary energy production and consumption respectively in 2019 [3]. Dominant role of coal in China's energy supply is expected to remain unchanged for decades [2]. Hence, it is necessary to promote clean and efficient utilization of coal to reduce the carbon dioxide (CO_2) emission. Coal-fired power plants based on steam-Rankine cycle have been widely utilized for a long history. It is known that thermal efficiency of the power plant increases by raising vapor temperature at the turbine inlet [4]. Nowadays, the state of art coal-fired power plant achieves around 48.12% net efficiency with steam parameters of 32.87 MPa/605 °C/623 °C/623 °C [5], in which 32.87 MPa is the maximum pressure at the turbine inlet, 605 °C is the steam temperature entering the high-pressure cylinder of the turbine, the first and second 623 °C refer to the steam temperatures entering the moderate-pressure cylinder and the low-pressure cylinder of the turbine, respectively. Water-vapor reacts with metal materials at ultra-high temperatures, introducing the difficulty to further explore the efficiency potential. Supercritical carbon dioxide cycle (sCO_2 cycle) uses sCO_2 consecutively flowing through various components to convert thermal energy into power. The sCO_2 cycle is believed to have higher

* Corresponding author.
E-mail address: xjl@ncepu.edu.cn (J. Xu).

https://doi.org/10.1016/j.enconman.2022.116166
Received 28 April 2022; Received in revised form 11 August 2022; Accepted 18 August 2022
Available online 31 August 2022

Nomenclature

B	coal consumption rate, kg/s
B_{cal}	coal consumption rate except unburned, kg/s
b_g	average standard coal consumption per kilowatt hour, g/kW·h
C	component cost, $
CRF	investment recovery factor
c_{ins}	the ratio of component materials and labor cost to component cost
d	diameter, m
e	specific exergy, kJ/kg
er	escalation rate over the years
E	exergy, kJelectricity generated, kW·h
f	friction coefficient
G	mass flux, kg/m^{2}s
h	enthalpy per unit mass, kJ/kg
I	exergy destruction, MW
l	length of component, m
m	mass flow rate, kg/s
P	pressure, MPa
Pr	Prandtl number
q	heat absorption per unit mass flow rate, kW/kg; heat loss percentage of boiler, %
Q	thermal load, MW; heating value, kJ/kg
Re	Reynolds number
r	ratio of heating or electric consumption discounted rate
s	entropy per unit mass, kJ/kg;
SP	scaling parameter of components for economic evaluation
T	temperature, °C
u	plant utilization factor
w	output/ input work per unit mass, kJ/kg
W	output/ input work, MW
x	split ratio

Greek symbols

φ	boiler heat retention coefficient
Δ	difference; absolute roughness of tubes, mm
ΔP	pressure drop, MPa
η	efficiency
ρ	density, kg/m^3
λ	thermal conductivity, W/(m·K)
ϕ	the ratio of the volume of i-th species to the total flue gas volume

Subscripts

0	environment
1, 2, 3…	state points
ar	received basis of the designed coal
ave	average
c	high temperature side
cal	calculated value
e	electric power
exg	exhaust flue gas
f	fluid; friction
j	type of components
fg	flue gas
fh	fly ash after coal fired
flame	theoretical combustion
h	high temperature side
i	inner of tube; inlet of medium temperature flue gas heater; the i-th species
net	net power out put
o	outer of tube; outlet of medium temperature flue gas heater
p	pipeline
sec	secondary
th	thermal

Abbreviation

AP	air preheater
C1	the main compressor
C1′, C2, C3	the auxiliary compressor
CTB	connect-top–bottom cycle
DRH	double reheating
EAP	external air preheater
FC	four compression cycle
FGC	flue gas cooler; a method to absorb residual flue gas heat which a flue gas cooler is arranged in boiler tail flue
FGR	flue gas recirculation
HTR	high-temperature recuperator
IC	intercooling
LCOE	levelized cost of electricity
LHV	lower heating value
LTR	low-temperature recuperator
MTR	mode-temperature recuperator
OEU	overlap energy utilization
PFM	partial flow mode
RC	recompression cycle
RH	reheating
RH1, RH2, RH3, RH4	reheater 1, reheater 2, reheater 3, reheater 4
SC	simple cycle
SH1, SH2	superheater 1, superheater 2
T1, T2, T3	turbine
TC	tri-compression cycle
TFM	Total flow mode

efficiency compared with steam-Rankine cycle, by elevating the main vapor temperature due to the weak chemical reaction rate between sCO_2 and metal materials [6].

In this section, we gave a short review on the general analysis of sCO_2 cycle without coupling heat source. Then, we summarized the key issues and solutions for sCO_2 coal-fired power plant. In the end of this section, we highlight the major contribution of the present paper.

The sCO_2 cycle was proposed in 1950 s [7]. Feher [8] investigated the simple recuperated cycle (SC) in 1967, consisting of a turbine, a heater, a recuperator, a compressor and a cooler. He discussed the mismatch between hot side fluid and cold side fluid in the recuperator. This mismatch introduces large temperature difference in the recuperator to lower the thermal efficiency of the system. To overcome this issue, Angelino [9] proposed the recompression cycle (RC), by adding an auxiliary compressor and a regenerator in the system. Since 1960 s, sCO_2 was not paid much attention, until in 2003, Dostal [10] introduced the sCO_2 cycle to nuclear power application. He noted that the thermal efficiency of sCO_2 cycle is higher than that of water-steam Rankine cycle with vapor temperature higher than 550 °C. Since then, many works have been done for sCO_2 cycles driven by nuclear energy [11-13], solar energy [14-17], waste heat [18-20], nature gas boiler [21,22] and coal-fired boiler [23-25]. These works focus on the optimization of the efficiency. Dostal [10] and moisseytsev et al [26,27] thought that RC is a promising cycle for the fourth generation nuclear power plant. For concentrated-solar power (CSP) plant, air-cooling was discussed for heat rejection from the cycle to the environment [15,28,29]. The air-cooling causes higher temperature at the compressor inlet and increases the compression work. Hence, inter-cooling (IC) was recommended to reduce the compression work [30,31]. Reheating (RH) was suggested to increase the thermal efficiency of the sCO_2 cycle [24,31]. Tri-compression sCO_2 cycle (TC) uses three compressors for thermal-power conversion. Moisseytsev et al. [27] pointed out that TC may not have the higher efficiency than RC, due to additional compression work used. Jiang et al. [32] thought that the TC performance may be improved due to the improved temperature match across the two sides of heat exchangers during the heat recovery process. Sun et al. [33] introduced synergetics to construct multi-compressions sCO_2 cycle. They reported that the thermal efficiencies are increased from 47.43% for RC to 49.47% for TC at the main vapor parameters of 550 ∘C/20 MPa.

Le Moullec [23] introduced the sCO_2 coal-fired power plant in 2013, in which the RC + DRH cycle is integrated with a tower type boiler. The sCO_2 coal-fired power plant was widely studied for a 1000 MWe capacity in China [24,34]. The cycle becomes complicated when coupling with the boiler heat source. Key issues and solutions are summarized as follows.

Flue gas energy absorption over entire temperature range (key issue 1): The distinct characteristic of boiler is that the flue gas energies over a wide range of temperature should be absorbed by the cycle. To achieve this target, flue gas cooler (FGC) was arranged in the tail flue to recover flus gas heat in low temperature range [35-37]. A portion of sCO_2 stream is extracted from a lower temperature point of the cycle, flows through the FGC to absorb flue gas heat, and returns to a higher temperature point of the cycle. Such application maintains the exit flue gas temperature to an acceptable level, keeping higher boiler efficiency, but decreases the cycle efficiency due to more heat added to the cycle [24]. Sun et al [38] proposed a connected-top–bottom sCO_2 cycle (CTB) to absorb flue gas energy over entire temperature range, in which flue gas energies in high, moderate and low temperature zones are absorbed by the top cycle, bottom cycle and air-preheater, respectively. Because the two cycles operate at different temperature zones, efficiencies exist between them. To fill the efficiency gap between the two cycles, Sun et al. [34] further proposed the overlap energy utilization (OEU) principle. An overlap zone in high flue gas temperature zone is set. Flue gas energy in this region is not only absorbed by the top cycle, but also by the bottom cycle. Hence, the overall system efficiency is optimized [34].

Pressure drop penalty effect (key issue 2): The flow rate of sCO_2 cycle is 6 ~ 8 times larger than that of steam Rankine cycle, causing extremely large pressure drop of boiler to decrease system efficiency, which is called the pressure drop penalty effect [24]. Large diameter (~100 mm) tubes of cooling wall decrease pressure drop [23,25], but worsen the heat transfer across the flue gas side and tube side, and introduces challenge in fabricating the cooling wall component [24]. Xu et al. [39] proposed the partial flow mode (PFM) to yield boiler module design, by which pressure drops for sCO_2 cycle can be decreased to a similar level as those of water-steam Rankine cycle.

Overheating of cooling wall (key issue 3): Compared with steam boiler, the inlet temperature of sCO_2 is 200 °C higher than that of water, and the heat transfer coefficient in tubes is about 5 kW/m^2K [40], much less than that of water. How to prevent the cooling wall from overheating is a key issue of sCO_2 boiler. Xiang et al [41] introduced flue gas recirculation (FGR) to reduce the furnace heat flux to decrease the cooling wall temperatures. Other efforts to suppress the cooling wall temperatures can be found in Refs. [42,43].

In summary, a practical sCO_2 cycle driven by boiler is complicated due to the following factors: (1) flue gas energy should be absorbed over the whole temperature range, (2) the cycle shall eliminate the pressure drop penalty, and (3) the temperatures of cooling walls shall be maintained in an acceptable level to keep the safety operation of the boiler. The solutions to overcome the above issues have been reported in the literature (see Table 1). It is noted that various references focus on the solution of specific issue. For example, Ref. [33] focusses on general sCO_2 cycle analysis without coupling heat source. Refs. [24,39] focus on the discussion of using partial flow mode to decrease pressure drops of boiler. Refs. [23,34,37,38,44] focus on the analysis using FGC, CTB and OEU to absorb flue gas energies over the entire temperature range. Even though the above works are reported, a question which needs to be answered is that what is the efficiency limit and how to reach the efficiency limit? The major contribution (or say the novelty) of the present paper is to propose a roadmap to reach the efficiency limit for sCO_2 coal-fired power plant. The roadmap is reflected in two levels. The first level considers general analysis of sCO_2 cycle. By comparing the cycle performances of RC, TC, TC + RH, TC + DRH (double reheating), and TC + DRH + IC consecutively, we conclude that TC + DRH + IC is applicable to reach the high efficiency of the system. The second level regards the sCO_2 cycle coupling with the boiler heat source, in which the OEU is used to absorb flue gas energies over entire temperature range, and the partial flow mode is used to decrease the pressure drops of boiler. Besides, cooling wall temperatures are controlled in an acceptable level. Therefore, the proposed roadmap not only reaches the efficiency limit, but also solved the thermal–hydraulic issues that are distinct for sCO_2 cycle driven by the boiler heat source.

The present work was divided into general sCO_2 cycle analysis (section 2, Figs. 1-4) and practical sCO_2 cycle analysis (section 3 and 4, Figs. 5-16). The proposed roadmap for efficiency improvement is to elevate average heat absorption temperature ($T_{ave,\ h}$) and lower average heat rejection temperature ($T_{ave,\ l}$). Results conclude TC achieves the second largest contribution for efficiency increment, after by the reheating technique. Then TC, DRH and IC are integrated as TC + DRH + IC in the coal fired power plant. After that, practical sCO_2 cycle are conducted. Key issues and corresponding solutions existing in practical sCO_2 power plant are analyzed and reviewed first, and specific implementation process in this paper is performed, then a numerical model is developed, subsequently, a comprehensive 1000 MWe sCO_2 coal-fired power plant conceptual design is finished. At last, the energy-exergy-economic evaluation analysis is developed to investigate the performance of the system. This work is of great significance to clear the development potential of sCO_2 coal-fired power plant.

Table 1
sCO_2 cycle studies for coal-fired power plant reported in the literature.

	General cycle configurations					Practical cycle configurations						comments
	RC	TC	RH	DRH	IC	FGC	CTB	OEU	PFM	TFM	FGR	
Ref.[33]	√	√	√	√								general approach for sCO_2 cycle
Ref.[24]	√			√	√	√			√			practical sCO_2 cycle analysis focusing on key issue 2
Ref.[39]	√		√					√	√	√		effect of power capacities focusing on key issue 2
Ref.[38]	√			√			√		√			sCO_2 cycle analysis focusing on key issue 1 using CTB
Ref.[34]	√			√	√			√	√			sCO_2 cycle analysis focusing on key issue 1 using OEU
Ref.[44]	√	√	√			√		√		√		sCO_2 cycle analysis focusing on key issue 1 by comparing OEU and FGC
Ref.[23]	√			√		√						conceptual design of a coal-fired power plant with FGC
Ref.[36]	√		√			√						sCO_2 cycle analysis focusing on key issue 1 using FGC
Ref.[37]	√		√	√		√						sCO_2 cycle analysis focusing on key issue 1 using FGC
This paper		√		√	√			√	√		√	comprehensively using various strategies to reach the maximum efficiency of the power plant

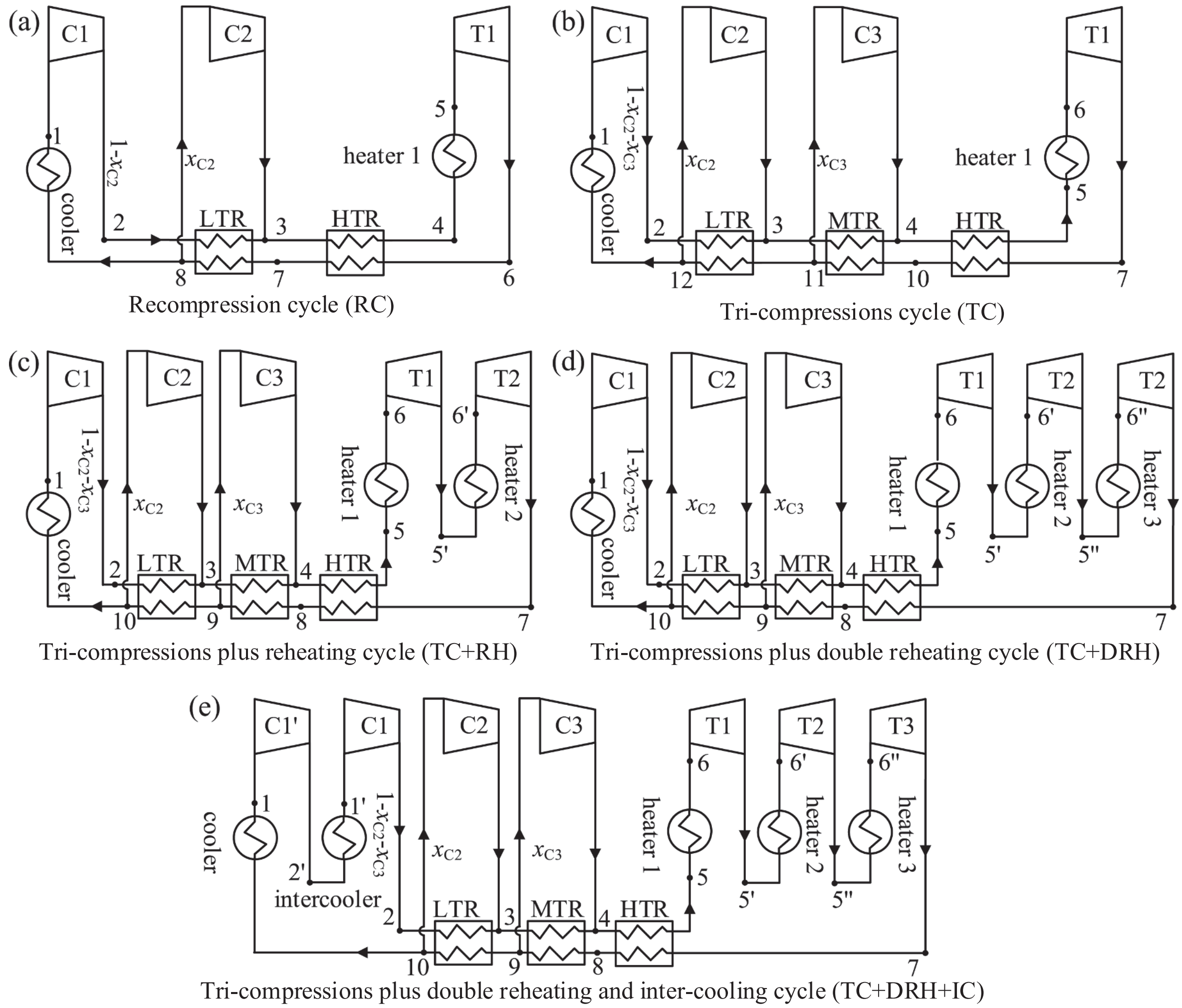

Fig. 1. sCO_2 cycle flow chart. (a) Recompression cycle (RC); (b) Tri-compression cycle (TC) which is replotted based on ref. [33], Copyright 2020, Elsevier; (c) Tri-compression plus reheating (TC + RH); (d) Tri-compression plus double reheating (TC + DRH); (e) Tri-compression plus double reheating and inter-cooling cycle (TC + DRH + IC).

2. Efficiency improvement for general sCO_2 cycle

RC cycle is the most classic sCO_2 cycle, widely applied for various heat sources for its higher efficiency, consisting of two compressors (C1 and C2), a turbine (T1), a low temperature recuperator (LTR) and a high temperature recuperator (HTR) (see Fig. 1a). Heat is added to the cycle via heater1 and heat rejection occurs in the cooler. Multi-reheating and multi-intercooling are adopted to raise the efficiency of Brayton cycle in literature, yet there is a lack of general approach. Inspired by the lack, Sun et al.[33] introduces synergetics to construct multi-compressions sCO_2 cycle, which can be thought as a sCO_2 Brayton cycle (A cycle) cooperating with another simple Brayton cycle SC. Such as TC (see Fig. 1b) can be thought as a RC cooperating with a SC. The SC dissipates extra heat to RC, not to environment, which ensures the SC to have an efficiency of 1. The internal heat recycling ensures TC to have an amplifying feedback. TC has two split-flow processes. It should be emphasized that the above conclusion is valid at optimal split ratio of flow, which also means that the two subsystems are cooperative to have no mixing induced exergy destruction. As the same way as TC, four-compressions sCO_2 cycle (FC) is formed by adding SC to TC, however, the efficiency increment is more obvious from RC to TC than that from TC to FC [33], as well, increasing compression stages not only narrows the heat absorption temperature range of cycle, but also complicates the cycle configuration. Hence, considering a trade-off of cycle efficiency increment and the cycle configuration complexity, TC is considered an ideal choice for the sCO_2 cycle power system.

RH is called as CO_2 is reheated in a heater before it enters the next turbine. As shown in Fig. 1c and 1d, the sCO_2 cycles are TC + RH and TC + DRH respectively, which TC + RH has two turbines of T1 and T2, TC + DRH for three turbines of T1, T2 and T3. RH is a technique used to increase the expansion work. As well, RH elevates the average heat absorption temperature $T_{ave,h}$ to gain the efficiency increment.

Intercooling (IC) is called as main compressor is divided into two compressors with an additional cooler between the two compressors. Fig. 1c shows TC + DRH + IC. An additional compressor C1′ and an intercooler are added between cooler and C1. IC is a technique used to decrease the compressor consumed power represented by reducing the enclosed *P-v* area. As the number of stages is increased, the compression process becomes nearly isothermal at the compressor inlet temperature. IC lowers the average heat rejection temperature $T_{ave,l}$ to gain the efficiency increment.

This section compared the contribution of tri-compression, reheating and intercooling techniques for efficiency improvement. The roadmap of efficiency improvement for general sCO_2 cycle is developed referenced to Carnot cycle. The general cycle analysis is helpful to develop an efficient concept design of practical sCO_2 power plant. Assumptions is necessary to start general cycle analysis, which are summarized as follows.

Pinch temperature difference is 10 °C in recuperators (LTR, MTR and HTR). Pressure drop in recuperators and heaters are neglected as it does

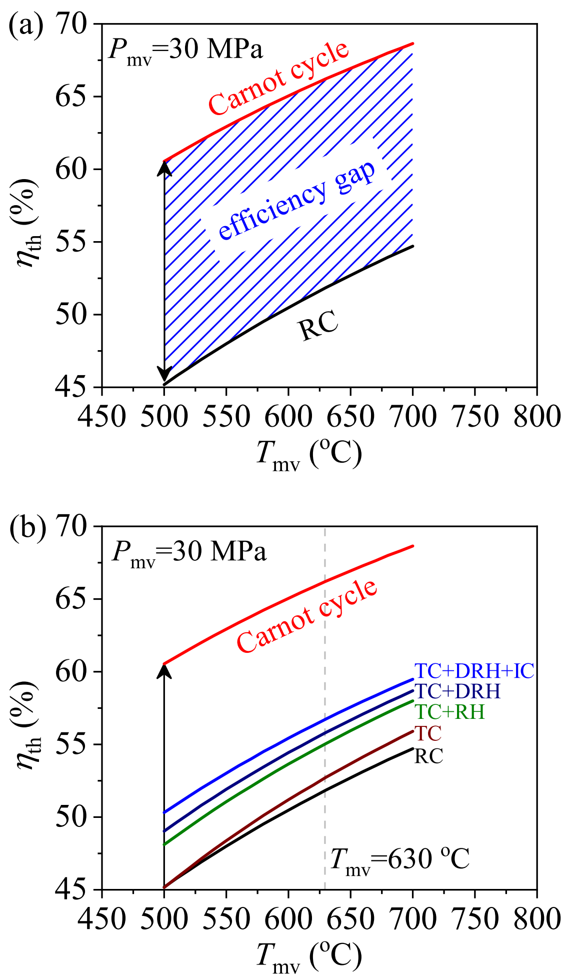

Fig. 2. sCO_2 cycle for efficiency improvement. (a) Efficiency gap between Carnot cycle and RC; (b) Efficiency improved by adding compression, reheating and intercooling.

not influence the major conclusion of general analysis of sCO_2 cycle. There are several mixing points in the cycle. No mixing-induced exergy destruction exists due to the same temperatures and pressures for mixing of different fluid streams. CO_2 physical properties come from NIST software REFPROP, which is widely used for cycle analysis.

Energy conservation and efficiency equations for various components of general sCO_2 cycle are summarized in Table 2. The cycle computation procedure could refer to ref. [24] and [33]. The input parameters include CO_2 temperature and pressure at turbine T1 inlet and main compressor C1 inlet, pinch temperature in recuperators, and isentropic efficiencies of compressors and turbines. Table 3 lists important parameters for general cycle computation.

The efficiency of Carnot heat engine is the highest, of which all heat engines operating between the two thermal energy reservoirs at temperatures T_l and T_h. Carnot efficiency refers to.

$$\eta_{th} = 1 - \frac{T_h}{T_l} \tag{1}$$

For a thermodynamic cycle with varied temperature of heating and cooling processes, Eq. (1) is modified as.

$$\eta_{th} \approx 1 - \frac{T_{ave,h}}{T_{ave,l}} \tag{2}$$

Where average heat absorption temperature $T_{ave,h}$ and the average heat rejection temperature $T_{ave,l}$ are determined by [34].

$$T_{ave,h} = \frac{\sum_{i=1}^{N} Q_{h,i}}{\sum_{i=1}^{N} \Delta S_{h,i}} = \frac{\sum_{i=1}^{N} m_i \left(h_{h,out,i} - h_{h,in,i}\right)}{\sum_{i=1}^{N} m_i \Delta s_{h,i}} \tag{3}$$

$$T_{ave,l} = \frac{\sum_{i=1}^{M} Q_{c,i}}{\sum_{i=1}^{M} \Delta S_{c,i}} = \frac{\sum_{i=1}^{M} m_i \left(h_{c,out,i} - h_{c,in,i}\right)}{\sum_{i=1}^{M} m_i \Delta s_{c,i}} \tag{4}$$

In Eqs. (3) and (4), Q is the heat transfer load, m is the mass flow rate of cycling fluid, i means the ith heating or cooling process, for example, 56 is a heating process (i = 1), 5′6′ is heating process (i = 2), 5‴6″ is another heating process (i = 3) (see Fig. 1), N and M are the number of heating and cooling process, respectively, the subscript in and out represent inlet and outlet states for i-th process, the subscripts h and c mean heating process and cooling process, respectively.

Fig. 2a shows that 15% efficiency gap is existed between RC and Carnot cycle at the main vapor pressure P_{mv} = 30 MPa. Fig. 2b shows the efficiency gap gradually decreases as the cycle configuration optimization path of TC, TC + RH, TC + DRH and TC + DRH + IC. $T_{ave,h}$ and $T_{ave,l}$ are used to explain the reason of efficiency increment.

Fig. 3 shows the T-s figure of different cycles at 30 MPa/630 °C turbine T1 inlet conditions, $T_{ave,h}$ and $T_{ave,l}$ are marked using red and blue dotted line respectively. TC has $T_{ave,h}$ of 532.5 °C, which is larger than 509.1 °C of RC. Correspondingly, the cycle efficiency is increased from 51.40% of RC to 52.73% of TC. TC + RH has $T_{ave,h}$ of 578.6 °C, which is larger than 532.5 °C of TC at the same calculation conditions (see Fig. 3c), correspondingly, the cycle efficiency is increased from 52.73% of TC to 55.05% of TC + RH. As the number of reheating stages is increased, $T_{ave,h}$ could be further elevated. Fig. 3d shows TC + DRH could obtain another 0.75% efficiency addition versus TC + RH. As shown in Fig. 3d and 3e, TC + DRH + IC has $T_{ave,l}$ of 39.6 °C, which is smaller than 46.4 °C of TC + DRH at the same calculation conditions, correspondingly, the cycle efficiency is increased from 55.80% of TC + DRH to 56.73% of TC + DRH + IC.

Fig. 4 compares the contribution for efficiency increment of TC, RH, DRH and IC, among which TC achieves the second largest contribution with 1.33% efficiency increment, after the reheating technique with 2.32% efficiency increment. TC and RH is strongly recommended for practical applications. Besides, IC and DRH make the comparable efficiency increment of 0.93% and 0.75%, respectively, which are recommended to further increase the efficiency after RH and TC. In all, considering a trade-off of cycle efficiency improvement and the cycle configuration complexity, though 9% efficiency gap between TC + DRH + IC and Carnot cycle existed (see Fig. 2b), it is not recommended to raise the cycle efficiency by increasing the number of compression, reheating and intercooling stages.

3. The sCO_2 coal-fired power plant

3.1. Key issues coupled with boiler

sCO_2 coal-fired power plant is a complex system. Once sCO_2 cycle is used for coal fired power plant, key issues are summarized as follows [24]. (i) It is difficult to recover the flue gas heat over a very wide temperature range of 1500–120 °C. (ii) Ultra-large pressure drop of sCO_2 boiler occurs to suppress system efficiency with conventional boiler design. (iii) Significantly higher inlet temperature of sCO_2 boiler leads to the cooling wall over temperature.

3.1.1. Flue gas energy absorption over entire temperature range

In the paper, OEU was adopted to recover flue gas energy over entire temperature range. The specific implementation process of OEU is illustrated by the 1000 MW sCO_2 coal-fired power plant, which both top cycle and bottom cycle apply TC + DRH + IC (see Fig. 5a and 5b), but an external air preheater (EAP) recycles extra heat of bottom cycle to the boiler. Fig. 5c shows the combine cycle after performing components sharing of top and bottom cycle. The components sharing technique is

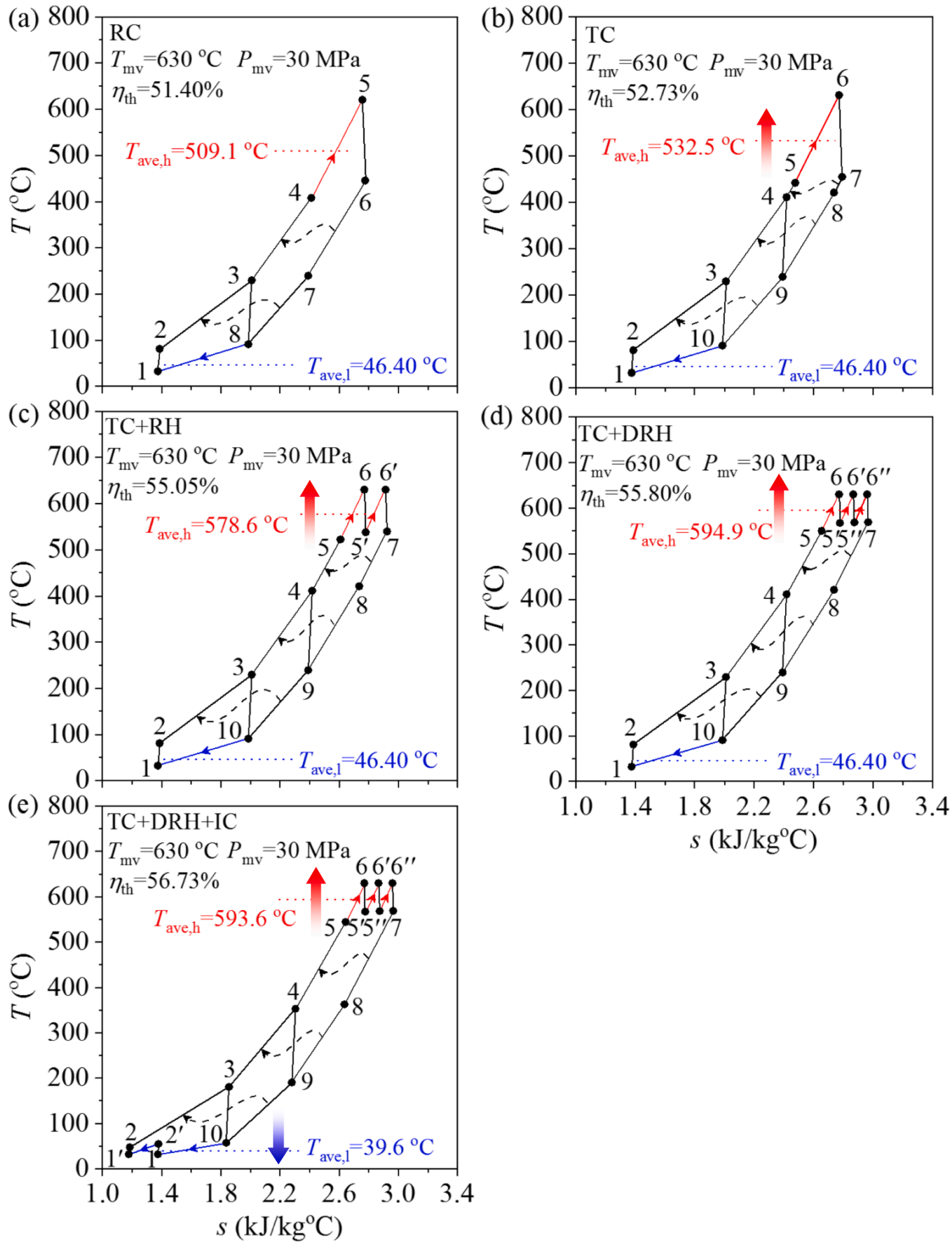

Fig. 3. Average absorption temperature $T_{ave,h}$ and average release temperature $T_{ave,l}$ of different sCO$_2$ cycle. (a) RC; (b) TC; (c) TC + RH; (d) TC + DRH; (e) TC + DRH + IC.

applied to simplify the system layout based on the similar CO_2 pressures and temperatures in some components of the two cycles, For example, T_6 and $T_{5'}$ across T1 in top cycle equal to T_{6b} and $T_{5'b}$ across T1b in bottom cycle. Hence, T1b in bottom cycle can be combined into T1 in top cycle. $T_{fg,i}$, $T_{fg,o}$ and $T_{fg,ex}$ are called the interface temperatures among the three regions of flue gas energies. Heaters 1, 2, 3 and 4b are responsible for the extraction of high temperature flue gas energy. Heater 4a', heater 4a'' and AP2 account for the extraction of moderate temperature flue gas energy. Low temperature flue gas energy is absorbed by AP1 only. As shown in Fig. 5c and 6d, two overlap zones are set in high and moderate temperature region, respectively. Overlap zone 1 covers the flue gas temperature range from $T_{fg,i} + \delta_1$ to $T_{fg,i}$, where δ_1 is called the deviation temperature. Flue gas energy in this subzone is not only absorbed by top cycle, but also by bottom cycle, represented by heater 4b and heater 3. The overlap energy utilization ensures no efficiency gap between top cycle and bottom cycle. Fig. 5e shows the *T*-s curve of top cycle and bottom cycle. Overlap zone 2 covers the flue gas temperature range from $T_{fg,i}$ to $T_{fg,i} + \delta_2$, flue gas energy in this subzone absorbed by heater 4a' and AP2 with the parallel arrangement, which increases the capability to extract moderate/low temperature flue gas energy, decreasing outlet flue gas temperature and raising boiler efficiency [34].

3.1.2. sCO$_2$ boiler module design

The cycling mass flow rate m is scaled as $m = Q/\Delta h$, where Q is the

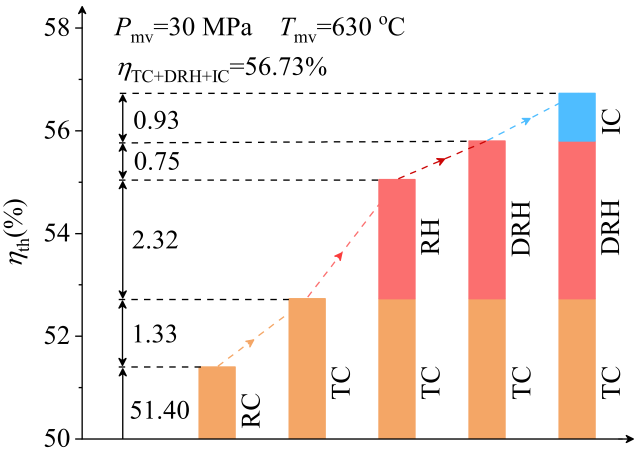

Fig. 4. Efficiency improvement of multi-compression, reheating and inter-cooling at the main vapor parameters of 30 MPa / 630 °C.

rate of heat absorption and Δh is the specific enthalpy difference of working fluid entering and leaving a boiler. Because CO_2 has much smaller Δh than water-steam under similar condition, m is significantly large, causing extremely large boiler pressure drop to decrease system efficiency, which is called the pressure drop penalty effect. To overcome this issue, many researchers considered using larger tube diameters to reduce pressure drop, but worsen the heat transfer across the flue gas side and tube side, and introduces challenge in fabricating the cooling wall component. Xu et al [24] proposed the PFM to yield boiler module design. Fig. 6 exhibits the two flow modes. Total flow mode (TFM) is a series connection mode. For PFM, The total flow rate is divided into two parallel lines, each having half tube length $L/2$ and half flow rate $m/2$, reducing pressure drop to 1/8 of that with the TFM. The total CO_2 flow rate, total tube length, and total heat absorption of two modes remain constant. Fig. 5c shows the sCO_2 cycle driven by a boiler with Heaters 1, 2, 3, 4a and 4b. PFM is applied to yield boiler module design shown in Fig. 6. Heater1 in Fig. 5c, as the main heating process, is decoupled into two branches in parallel, each branch accounts for half flow rate, in which Part 1 and SH1 are connected with each other as one branch, Part 2 and SH2 as the other branch. Similarly, Heater 2, as the reheating process, is decoupled into (Part 3 + RH1) and (Part 4 + RH2) two parallels. Heater 3, as double reheating process, is decoupled into RH3 and RH4 in parallel connection.

3.1.3. Flue gas recirculation

For coal-fired boiler, when CO_2 is used instead of water, significant change happens on the heat transfer performance. Such as, the temperature of CO_2 entering the boiler furnace increases by 100–200 °C [41] and the heat transfer coefficient of sCO_2 is only about 1/3 of that of water [41], which results in over-temperature of heating exchanger. Flue gas recirculation, extracting part of low temperature flue gas from tail flue to the furnace, is proposed to enhance the heat transfer and reduce the heat flux density of the furnace, which could relieve the heat transfer deterioration. Meanwhile, flue gas recirculation could also reduce the generation of thermal NO_x and inhibit coke formation. The technique is adopted in this paper. Fig. 7 shows specific implementation, which a portion of low temperature flue gas is recirculated from the inlet of low temperature flue gas region, correspondingly inlet of AP1 in Fig. 5c, and send it to the furnace.

3.2. Numerical model

Fig. 9 shows the computation scheme, consisting of two subroutines. Once initial parameters are given (see Table 4), pressure drops in various heaters of boiler are assumed, then the thermodynamic cycle subroutine is called. Parameters of state points, components heat load/work, coal consumption rate and thermal efficiency are obtained after thermodynamic cycle subroutine finished. And then, distribute heat load of heater components in boiler to continue sCO_2 boiler subroutine. Pressure drop in heaters are obtained and calculate residual value of pressure drops in Heaters 1, 2and 3. The iteration computation is stopped until the residual value is smaller than a setting value. At last, the energy, exergy and economic evaluation is further conducted to analyze the system comprehensively.

The coal-fired power plant is a very complicated system. All the calculation schemes are reflected as the source code built by the present authors using the Matlab software platform. The proposed system adopts TC + DRH + IC cycle configuration. Overlap energy utilization is utilized to recover the flue gas heat over the whole temperature range. The proposed cycle also integrates the module boiler design to suppress the pressure drop penalty effect, and the flue gas recirculation to keep the heater surface temperature in an accepted level. Following assumptions are made: (i) steady system operation; (ii) CO_2 physical properties come from NIST software REFPROP, which is widely used for cycle analysis. (iii) no mixing-induced exergy destruction exists due to the same temperatures and pressures for mixing of different fluid streams. (iv) heat loss for boiler and pipe heat loss is considered, but neglected for other components.

3.2.1. Computation of sCO_2 cycle

Thermodynamic parameters at various state points are calculated as Table 5. Fig. A1 in appendix shows the computation scheme of cycle thermodynamic calculation. TC has two split flow processes as the cycle consists of three compressors and three regenerators. Partial flow rate flows through each compressor are 1-x_{C2}-x_{C3} in C1, x_{C2} in C2 and x_{C3} in C3. It should be emphasized that TC shows the best performance only at optimal split ratio of flow, the two subsystems are cooperative to have no mixing induced exergy destruction. The optimal split ratio are calculated as the following set of equations.

$$\begin{cases} x_{C1} = 1 - x_{C2} - x_{C3} \\ (1 - x_{C2} - x_{C3})(h_3 - h_2) = (1 - x_{C3})(h_9 - h_{10}) \\ (1 - x_{C3})(h_4 - h_3) = (h_8 - h_9) \end{cases} \tag{5}$$

The cycle computation needs to deal with overlap energy utilization. The flue gas energy is divided into high, moderate and low temperature region by two junction temperatures of flue gas, $T_{fg,i}$ and $T_{fg,o}$. Specified by the pinch temperature difference, $T_{fg,i}$ and $T_{fg,o}$ are related to the CO_2 temperatures in tube side with $T_{fg,i} \geqslant T_{CO2} + 40$ and $T_{fg,o} \geqslant T_{CO2} + 20$ at corresponding points. Since part of recirculating flue gas with the ratio of x_{rec} is extracted to send to the furnace, the flue gas flow rate flowing through high and moderate temperature region is scaled as $1+x_{rec}$ (x_{rec}=27% in the paper). Thermal load conservation of three regions are.

$$\begin{cases} \varphi B_{cal}(1 + x_{rec})(h_{flame} - h_{fg,i}) = Q_{heater1} + Q_{heater2} + Q_{heater3} + Q_{heater4b} \\ \varphi B_{cal}(1 + x_{rec})(h_{fg,i} - h_{fg,o}) = Q_{heater4a} + Q_{AP2} \\ \varphi B_{cal}(h_{fg,i} - h_{fg,ex}) = Q_{AP1} \end{cases} \tag{6}$$

where h is the flue gas enthalpy, φ is the boiler heat retention coefficient, $\varphi = 1\text{-}q_5/(100\eta_{boiler} + q_5)$, η_{boiler} is the boiler efficiency calculated by the anti-balance method and q_5 is a component of heat loss due to heat dissipation to environment, which can be determined by Ref. [45]. B_{cal} is coal consumption rate except unburned, called calculated coal consumption.

$$B_{cal} = B\left(1 - \frac{q_4}{100}\right)B = \frac{q_{total} m_{CO_2}}{Q_{LHV}\eta_{boiler}} \tag{7}$$

where B is coal consumption rate, q_4 is a component of heat loss due to unburned carbon, q_{total} is total heat absorption per unit mass flow rate of CO_2, m_{CO_2} is the total mass flow rate of CO_2, Q_{LHV} is the low heating value of design coal per unit mass (see Table 6).

Heater 4a is decoupled into heater 4a' and heater 4a'', arranged in the tail flue, to absorb the moderate flue gas energy. $Q_{heater4a}$ is.

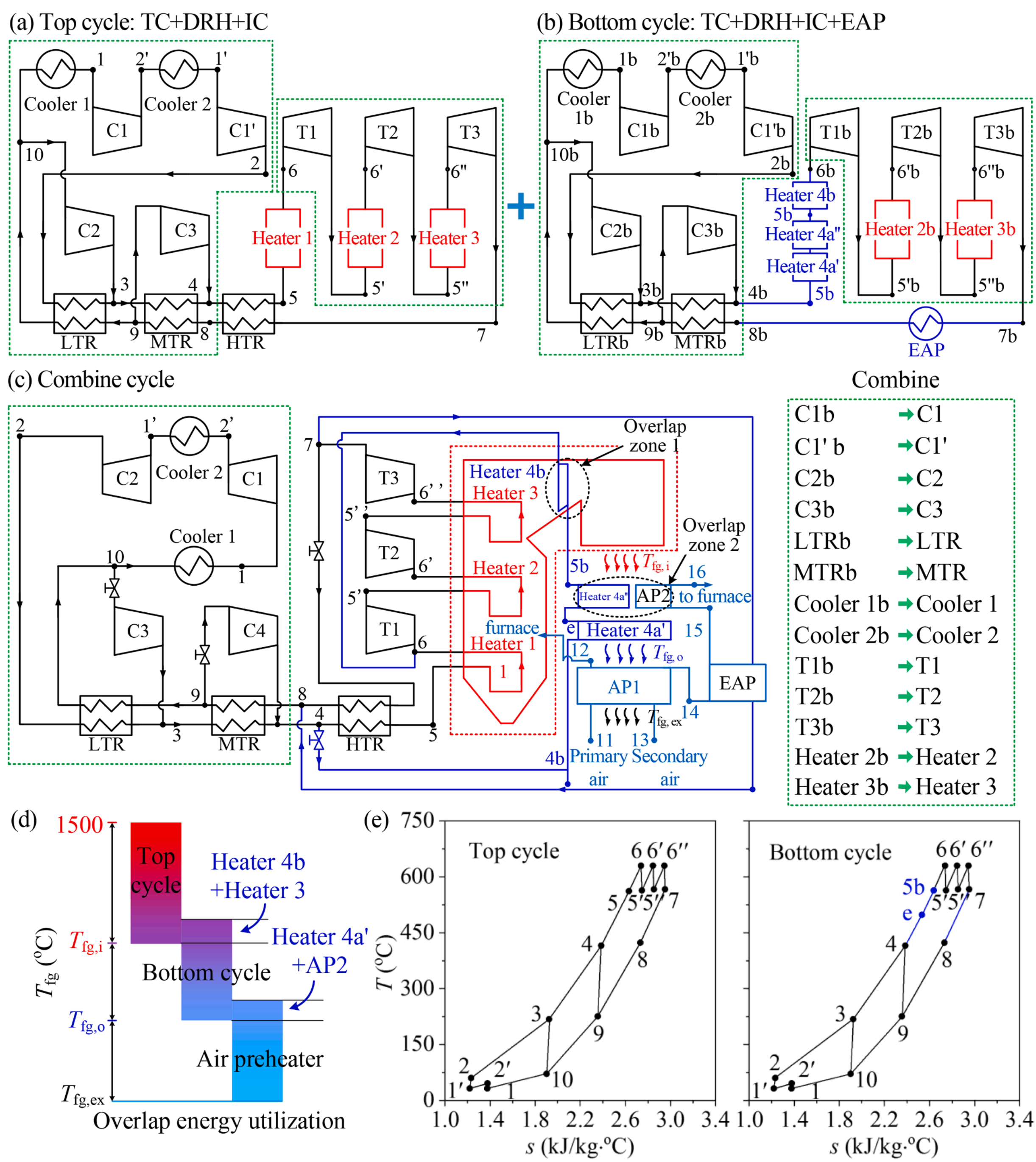

Fig. 5. sCO$_2$ cycle based on overlap energy utilization. (a) top cycle; (b) bottom cycle; (c) combined cycle after components sharing; (d) overlap energy utilization, replotted based on Ref.[39]; (e) *T*-s curve of top cycle and bottom cycle.

$$Q_{\text{heater4a}} = x_{\text{heater }4} m_{\text{CO2}}(h_6 - h_4) \tag{8}$$

Thermal efficiency η_{th} of the cycle is calculated as:

$$\eta_{\text{th}} = \frac{w_{\text{net}}}{q_{\text{total}}} \tag{9}$$

$$w_{\text{net}} = (w_{\text{T1}} + w_{\text{T2}} + w_{\text{T3}}) - (w_{\text{C1}'} + w_{\text{C1}} + w_{\text{C2}} + w_{\text{C3}}) \tag{10}$$

$$q_{\text{total}} = (1 - x_{\text{heater 4}})(h_6 - h_5) + x_{\text{heater 4}}(h_6 - h_4) + (h_{6'} - h_{5'}) + (h_{6''} - h_{5''}) - x_{\text{EAP}}(h_7 - h_8) \tag{11}$$

$$m_{\text{CO}_2} = \frac{W_{\text{net}}}{w_{\text{net}}} \tag{12}$$

where w_{net} is net power per unit mass flow rate of CO$_2$, x_{Heater4} is the ratio of flow rate in heater4a or heater4b to the total flow rate, x_{EAP} is the ratio of flow rate in EAP to the total flow rate, W_{net} is power capacity (W_{net}=1000 MW in the paper).

3.2.2. Computation of sCO$_2$ boiler

The proposed cycle driven by a boiler with heaters 1, 2, 3, 4a and 4b, in which heaters 1, 2 and 3 are decoupled into several heater components (see Fig. 6). The energy relationship are:

$$\begin{cases} Q_{\text{heater1}} = Q_{\text{part1}} + Q_{\text{part2}} + Q_{\text{SH1}} + Q_{\text{SH2}} \\ Q_{\text{heater2}} = Q_{\text{part3}} + Q_{\text{part4}} + Q_{\text{RH1}} + Q_{\text{RH2}} \\ Q_{\text{heater3}} = Q_{\text{RH3}} + Q_{\text{RH4}} \end{cases} \tag{13}$$

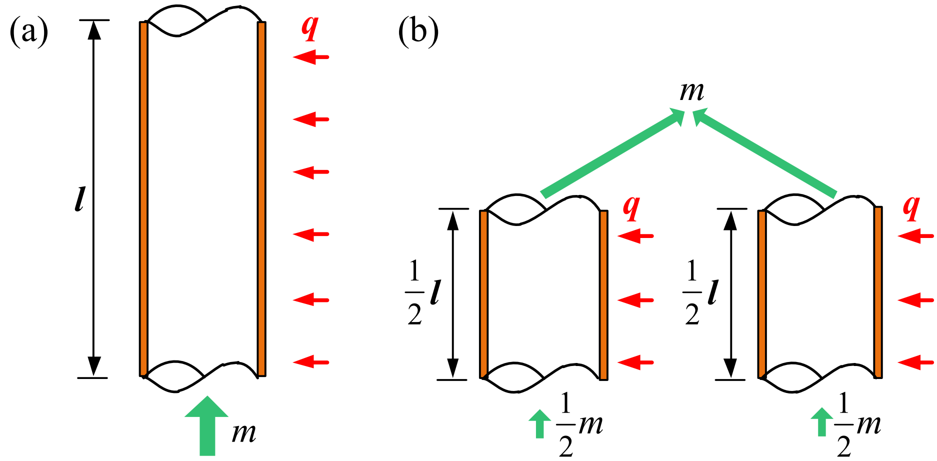

Fig. 6. Two flow modes. (a) total flow mode; (b) partial flow mode. This figure is cited from Ref. [39]. Copyright 2020, Elsevier).

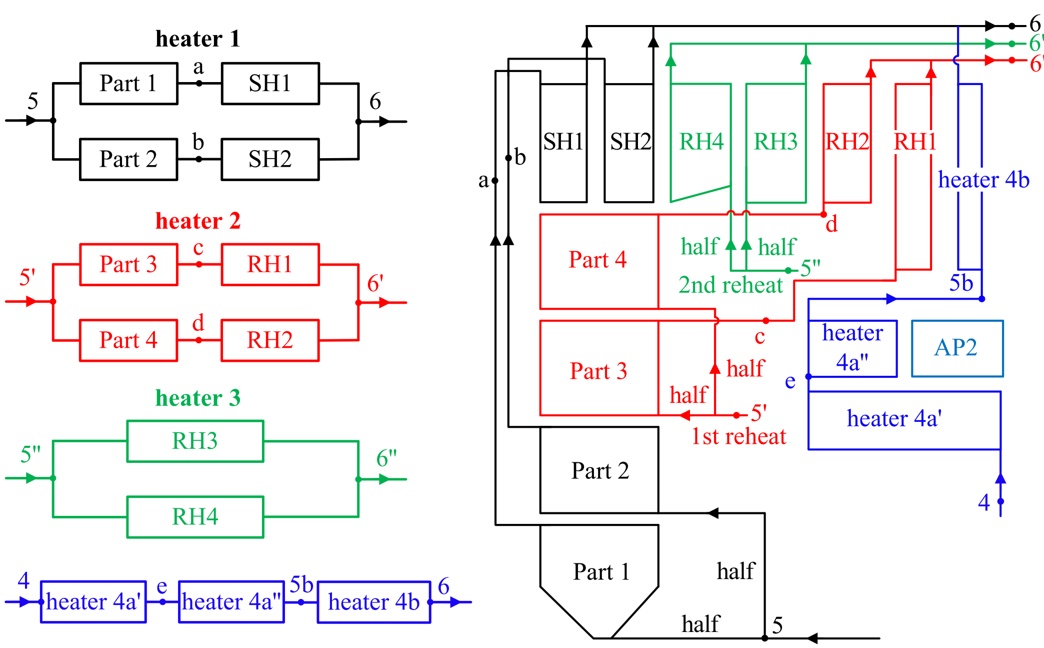

Fig. 7. sCO_2 boiler module design. This figure is replotted and modified from Ref. [40.

Pressure drops in boiler tubes consists of components of friction (ΔP_f), gravity (ΔP_g) and acceleration (ΔP_a).

$$\Delta P = \Delta P_f + \Delta P_g + \Delta P_a \tag{14}$$

$$\Delta P_f = \int_{z_{j-1}}^{z_j} \frac{f}{d_i}\frac{G^2}{2\rho}dz, \quad \Delta P_g = \int_{z_{j-1}}^{z_j} \rho g dz, \quad \Delta P_a = G^2\left(\frac{1}{\rho_o} - \frac{1}{\rho_i}\right) \tag{15}$$

where G and ρ are the mass flux and density, respectively, f is the friction coefficient [46].

$$f = \frac{1}{3.24\lg^2\left[\left(\frac{\Delta/d_i}{3.7}\right)^{1.1} + \frac{6.9}{Re}\right]} \tag{16}$$

where Δ is the absolute wall roughness, $\Delta = 0.012$ mm for stainless-steel tubes [47].

The boiler efficiency η_{boiler} is calculated by the anti-balance method [48]:

$$\eta_{boiler} = 1 - (q_2 + q_3 + q_4 + q_5 + q_6) \tag{17}$$

whereq_2,q_3,q_4, q_5 and q_6 are the ratio of heat losses due to exhaust gas, unburned gases, unburned carbon, heat dissipation to environment and physical heat loss of ash to the input energy of coal.q_3,q_4, q_5 and q_6 depend on boiler type and coal type (see Table 7 for specific values). q_2 is the biggest among the five ratios of boiler heat losses, calculated as:[45].

$$q_2 = \frac{Q_2}{Q_r}, \quad Q_2 = B_{cal}\left(h_{exg} - h_{ca}\right)\left(1 - \frac{q_4}{100}\right) \tag{18}$$

where Q_2 is the heat loss due to exhaust gas, h_{exg} is the exhaust gas enthalpy per unit mass coal, h_{ca} is the air enthalpy per unit mass coal at environment temperature, Q_r is the energy brought into boiler by coal, hot air and recirculating flue gas.

$$Q_r = B_{cal}\left(Q_{LHV} + h_{sec,ha} + x_{rec}h_{fg,o}\right) \tag{19}$$

where $h_{sec,ha}$ is the secondary air flow enthalpy after heated by AP1, EAP

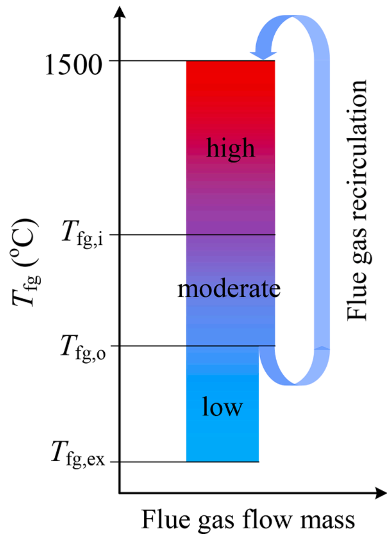

Fig. 8. Flue gas recirculation.

and AP2.

Fig. A2 in appendix shows the computation scheme of sCO_2 boiler and its thermal–hydraulic characteristic. The iteration calculation of furnace outlet temperature T_{fl} is performed to obtain boiler geometry parameters. Heating components of sCO_2 boiler includes both radiation modules and convective modules. The design methods are similar with water-steam boiler cited from Ref [49].

3.2.3. Exergy analysis

The input exergy of system equals to the chemical exergy of coal [44]:

$$E_{coal} = BQ_{LHV}\left(1.0064 + 0.1519\frac{H_{ar}}{C_{ar}} + 0.0616\frac{O_{ar}}{C_{ar}} + 0.0429\frac{N_{ar}}{C_{ar}}\right) \tag{20}$$

C_{ar}, H_{ar}, O_{ar} and N_{ar} are the ratios of C (carbon), H (hydrogen), O (oxygen) and N (nitrogen) on the received basis of designed coal, respectively (see Table 6).

Specific exergy per unit mass flow rate is calculated as $e = h - T_0 s$, where T_0 is the environment temperature, h and s are the enthalpy and entropy per unit mass flow rate. Exergy losses per unit mass flow rate in various components are shown in Table 5. The exergy loss in component j is $I_j = m_j i_j$ and the exergy balance equation can be expressed as.

$$\sum E_{in,j} = \sum E_{out,j} + W_j + I_j \tag{21}$$

where the expression on the left side of the equal sign is input exergy of component j, the output exergy is on the right side, consisting output exergy of CO_2, output work W_j and exergy lossI_j.

Boiler is a complicated system, considering as a whole component, boiler exergy loss I_{boiler} is.

$$I_{boiler} = E_{coal} - E_{out,boiler} \tag{22}$$

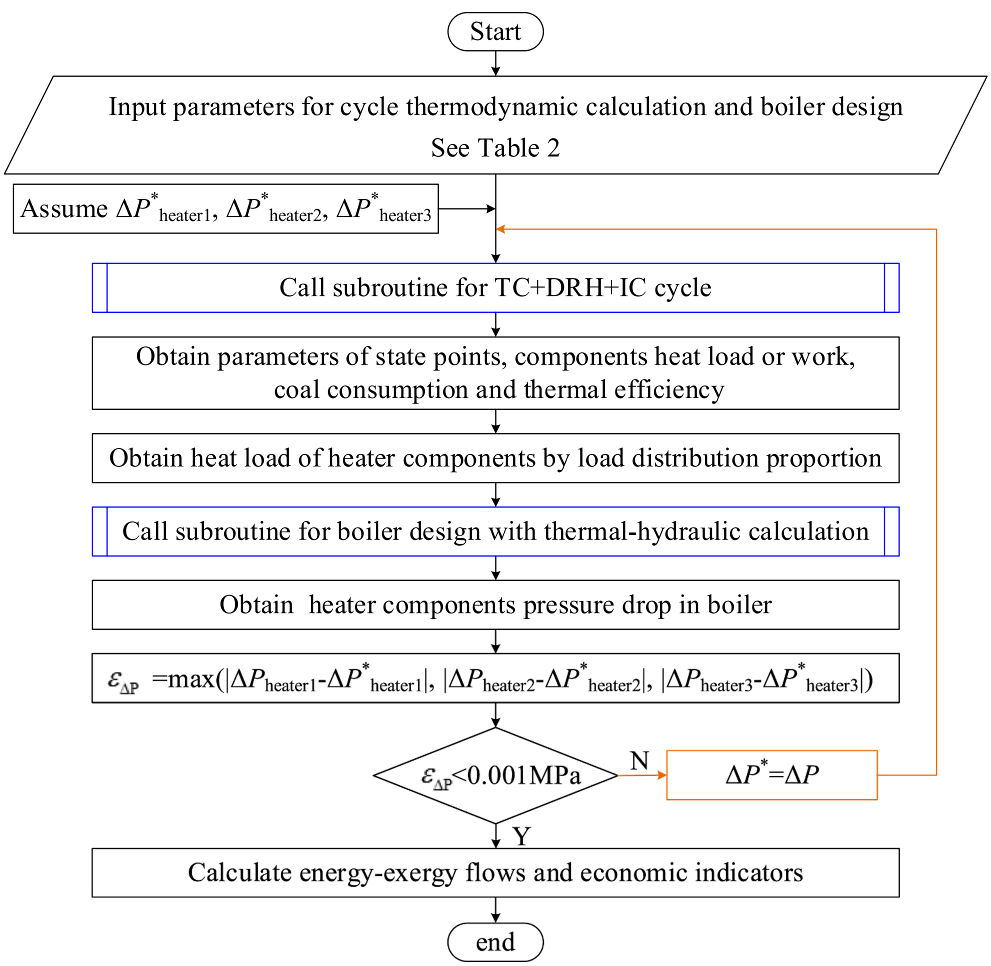

Fig. 9. Calculation scheme for the sCO_2 system.

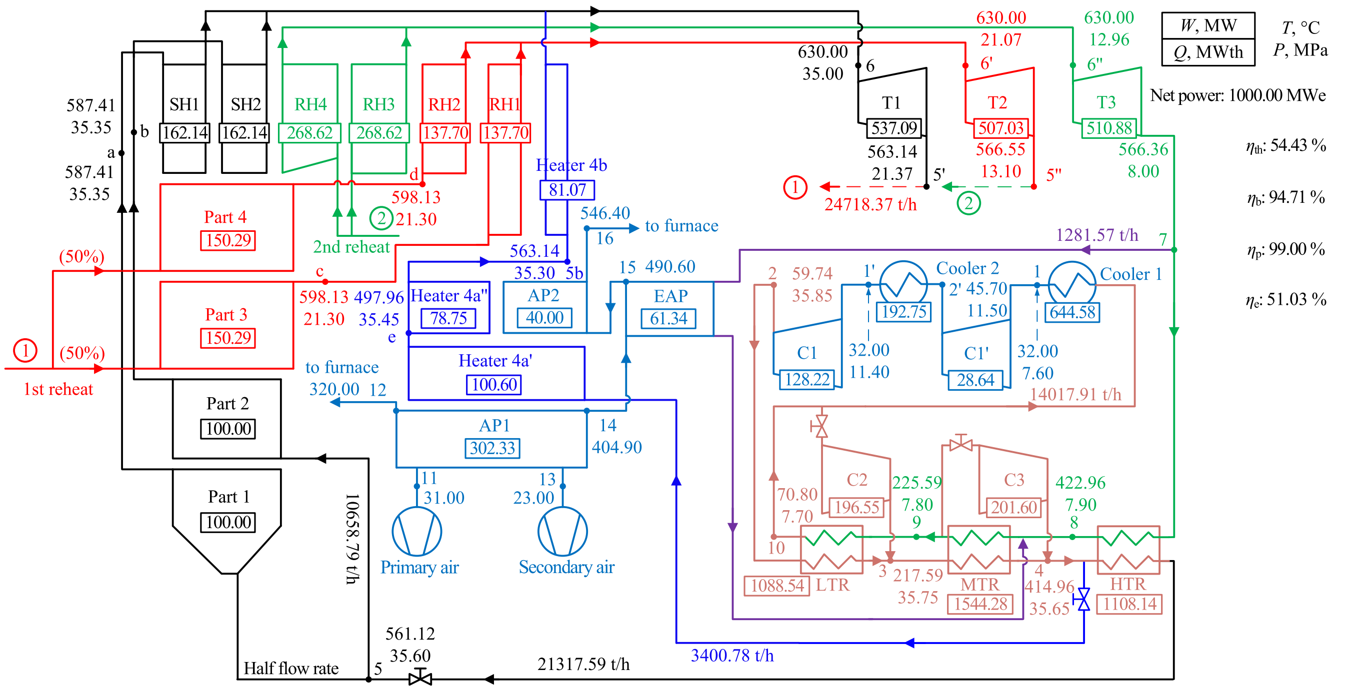

Fig. 10. sCO_2 power plant (TC + DRH + IC cycle, partial flow strategy to suppress pressure drops in various heaters, overlap energy utilization to absorb the whole range flue gas energy, main vapor parameters are 630 °C/35 MPa, 1000 MWe net power output, power efficiency η_e = 51.03%).

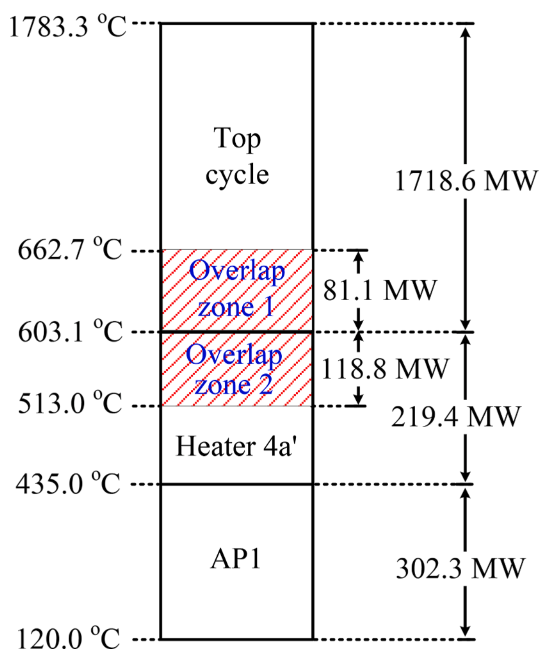

Fig. 11. Distributions of flue gas temperature and thermal loads.

$$E_{\text{out,boiler}} = m_{CO2}[(1 - x_{\text{Heater 4}})(e_6 - e_5) + x_{\text{Heater 4}}(e_6 - e_4) + (e_{6'} - e_{5'}) + (e_{6''} - e_{5''}) - x_{\text{EAP}}(e_7 - e_8)] \tag{23}$$

Considering the energy transfer and conversion in the boiler, I_{boiler} is.

$$I_{\text{boiler}} = I_{\text{com}} + I_{\text{heaters}} + I_{\text{mix}} + I_{\text{others}} \tag{24}$$

where I_{com} is exergy loss caused by combustion, I_{heaters} is exergy loss of heater components, I_{mix} is exergy loss in flue gas mixing process, I_{others} is the exergy loss caused by boiler heat losses.

Flue gas exergy e_{fg} is calculated as follows [44]:

$$e_{fg} = h_{fg} - T_0 s_{fg} h_{fg} = \sum_{i=1}^{M} \phi_i h_i + h_{fh} s_{fg} = \sum_{i=1}^{M} \phi_i s_i + s_{fh} \tag{25}$$

where s_{fg} is the entropy of flue gas per unit mass of coal, h_{fh} and s_{fh} are enthalpy and entropy of fly ash after unit mass coal fired, M are the species of flue gas, including CO_2, SO_2, N_2, O_2, H_2O steam, ϕ_i is the ratio of the volume of i-th species to the total flue gas volume.

Exergy efficiency η_{ex} of the system is:

$$\eta_{ex} = \frac{W_{\text{net}}}{E_{\text{coal}}} \tag{26}$$

3.2.4. Economic indicators

In order to assess economic aspects of the system, two economic indicators have been considered, coal consumption for power supply (b_g) and Levelized cost of electricity (LCOE).

The component cost model is presented as [50]:

$$C_k = a_k SP^{b_k} \times f_{T,k} \tag{27}$$

where k represents the component, C_k is the component cost, a_k and b_k are fit coefficients, SP is the scaling parameter, representing thermal heat duty for heaters and recuperators and shift power for compressors and turbines, $f_{T,k}$ is a temperature correction factor. Detailed cost correlation of components are shown in Table 8.

Besides, materials and direct labor costs needed for installation of components should be added to the equipment cost, $c_{\text{ins},k}$ is the ratio of kth component materials and labor cost to component cost C_k, the values are evaluated by NERL (see Table 8) [50]. The total investment cost of components C_{total} is calculated as.

$$C_{\text{total}} = \sum_{k=1}^{NC} (1 + c_{\text{ins},k}) C_k \tag{28}$$

b_g refers to the average standard coal consumption per kilowatt hour, which can be calculated by the following formula [51].

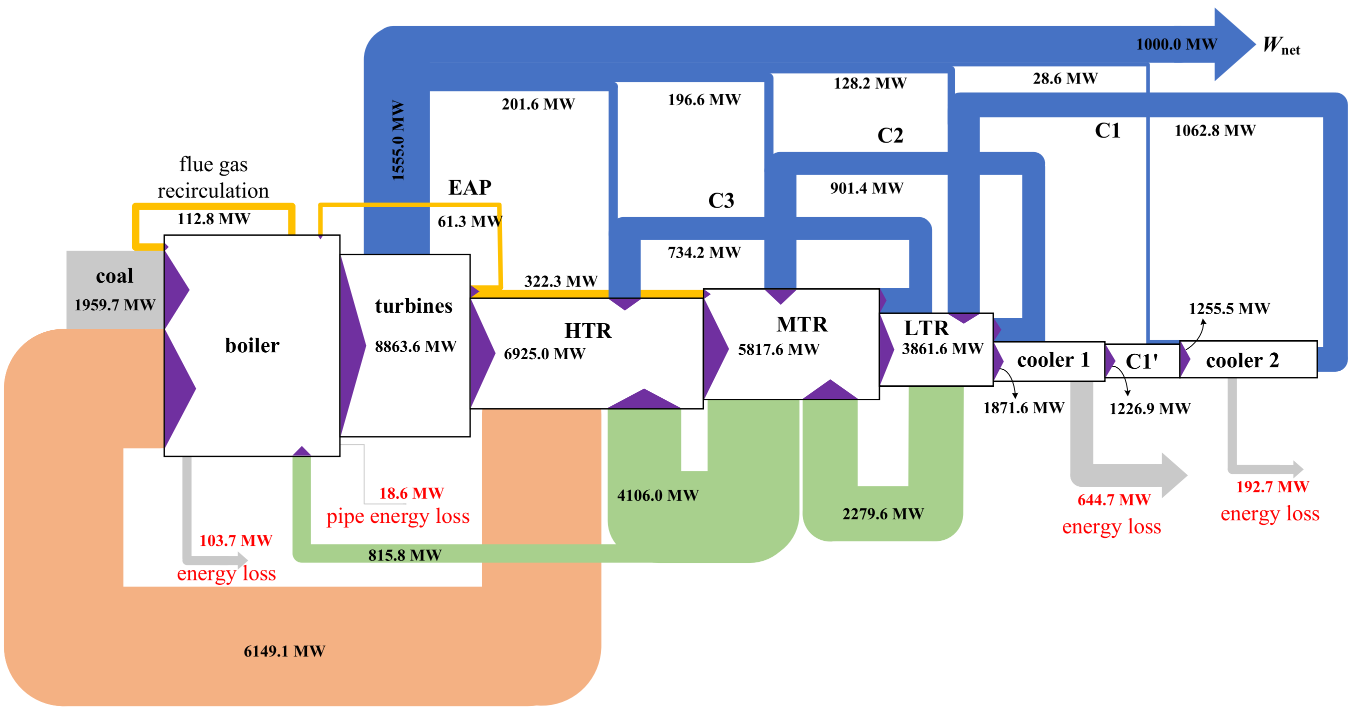

Fig. 12. Sankey diagram depicting the energy flowing through the coal-fired sCO_2 power plant (The width represents the amount of energy, the length does not have physical meaning).

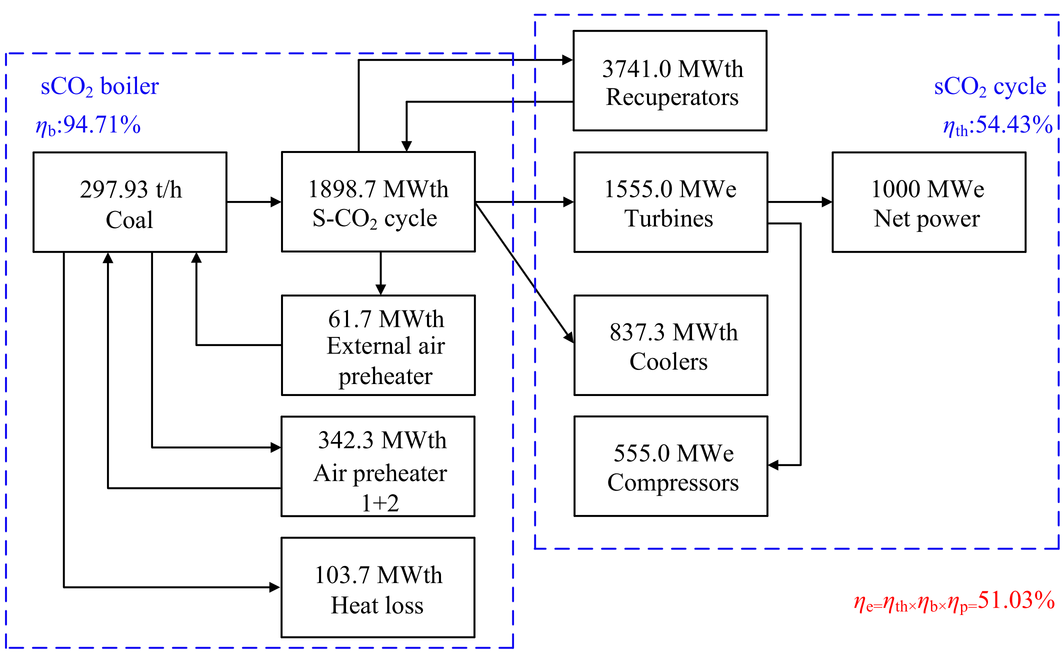

Fig. 13. Thermal load distribution of various components for the system.

$$b_g = \frac{B \times (1 - r_{heating})}{E_{gen} \times (1 - r_{house})} \tag{29}$$

where $r_{heating}$ is the heating ratio, r_{house} is auxiliary equipment electric consumption ratio, E_{gen} is the electricity generated.

LCOE refers to the ratio of the total cost to the total power output of the plant during its lifetime [52]. The total cost contains total investment cost of components C_{total}, the operation and maintenance cost C_{OM}, and fuel cost C_f. *CRF* is the investment recovery factor related to the discounted rate *r* and the lifespan of equipment *NY*. Plant utilization factor *u* is 0.85 (see Table 9). The parameter *OM* denotes the operation and maintenance costs per kW·h and the coefficient *er* is the escalation rate over the years. [53].

$$LCOE = \frac{CRF \times C_{total} + C_{OM} + C_f}{8760uW_{net} \times NY} \tag{30}$$

$$CRF = \frac{r(1+r)^{NY}}{(1+r)^{NY} - 1} \tag{31}$$

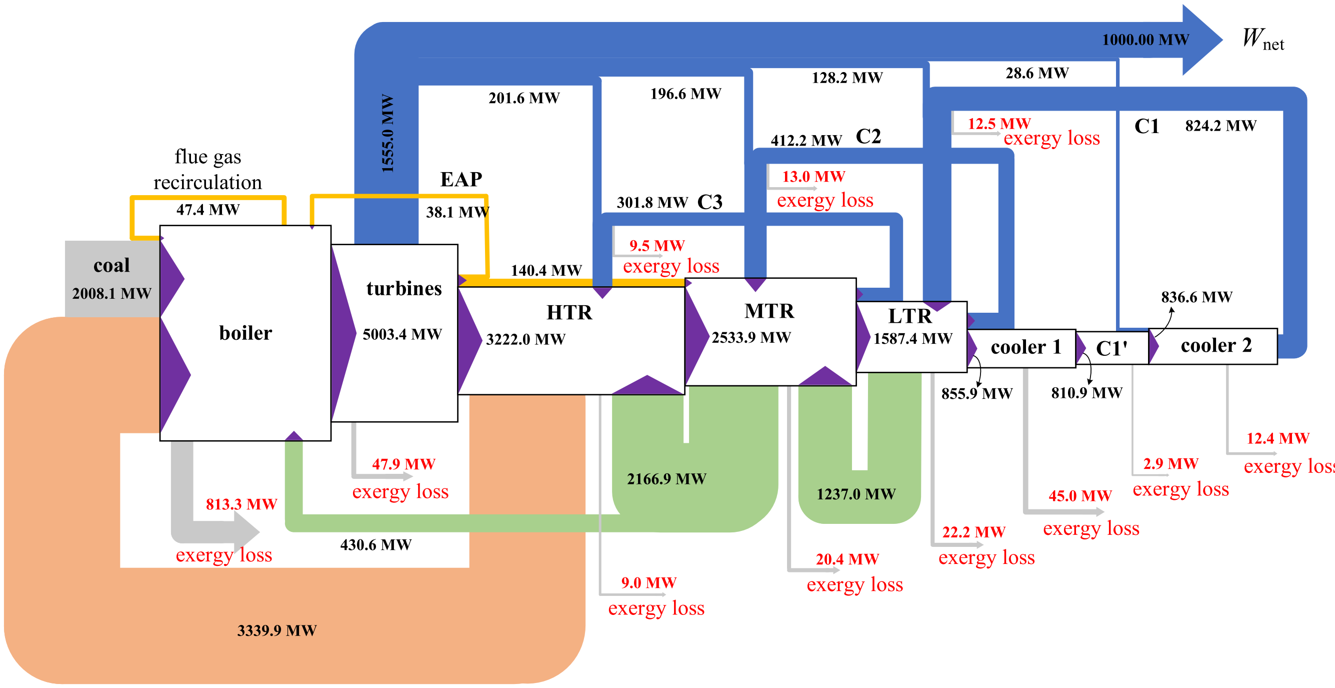

Fig. 14. Sankey diagram depicting the exergy flowing through the coal-fired sCO_2 power plant (The width represents the amount of exergy, the length does not have physical meaning).

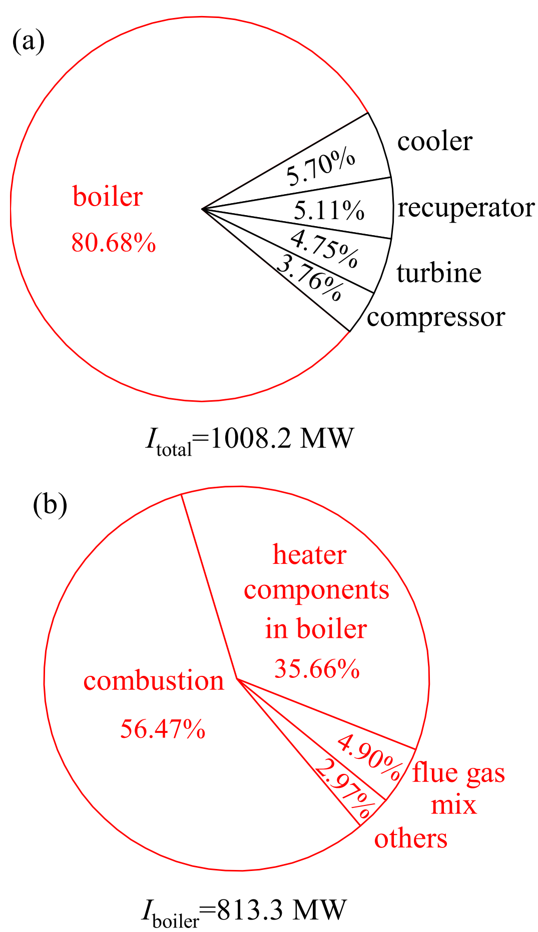

Fig. 15. Exergy destruction distributions in system components (a) and detail exergy destruction in boiler (b).

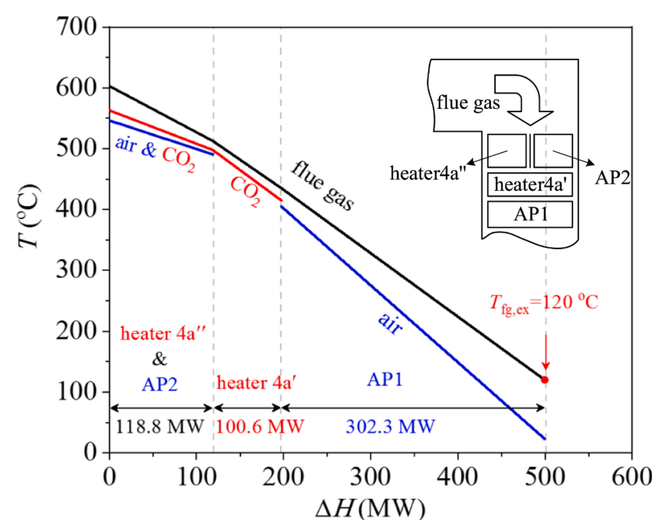

Fig. 16. *T*-Δ*H* curve for heat exchangers (heater 4a' and heater 4a'') and air preheaters (AP1 and AP2) operating in moderate and low temperature flue gas region.

$$C_{OM} = \sum_{m=1}^{NY} \frac{1000W_{net}(OM(1+er)^m)}{(1+r)^m} \tag{32}$$

$$C_f = 8.76 b_g W_{net} u \times NY \tag{33}$$

4. Results and discussion

4.1. The 1000 MW sCO_2 coal-fired power plant with the limit efficiency

Fig. 10 shows the 1000 MW sCO_2 coal fired power plant which reached the limit efficiency. The inlet and outlet temperature/pressure of each component is marked, and the thermal load/power is given. Anthracite coal was used, whose properties parameters are shown in

Table 2
Energy conservation and efficiency equations for various components of sCO_2 cycle [24].

Model	Energy relations	Subscripts explanation
turbine	$\eta_{t,s} = \frac{h_{t,in}-h_{t,out}}{h_{t,in}-h_{t,out,s}}$, $W_t = m_t(h_{t,in}-h_{t,out})$	t, in, out, s mean turbine, turbine inlet, turbine outlet, isentropic
heater	$Q_h = m_h(h_{h,out}-h_{h,in})$	h, in, out mean heater, heater inlet, heater outlet.
recuperator	$m_h(h_{h,in}-h_{h,out}) = m_c(h_{c,out}-h_{c,in})$	h, c, in, out mean hot side, cold side, inlet, outlet.
cooler	$Q_c = m_c(h_{c,in}-h_{c,out})$	c, in, out mean cooler, cooler inlet, cooler outlet.
compressor	$\eta_{c,s} = \frac{h_{c,out,s}-h_{c,in}}{h_{c,out}-h_{c,in}}$, $W_c = m_c(h_{c,out}-h_{c,in})$	c, in, out, s mean compressor, compressor inlet, compressor outlet, isentropic.
thermal efficiency	$\eta_{th} = \frac{W_t - \sum W_c}{Q_h}$	th, t, c, h mean thermal, turbine, compressor, heater.

Table 3
Parameters for generalized sCO_2 cycle calculation.

Parameters	Values
Inlet temperature of compressor	32 °C
Inlet pressure of compressor	7.6 MPa
Inlet temperature of turbine T_{mv}	630 °C
Inlet pressure of turbine P_{mv}	30 MPa
Isentropic efficiency of turbine [33]	93%
Isentropic efficiency of compressors [33]	89%
Pressure drop in regenerators and heaters [33]	0 MPa
Pinch temperature difference of regenerators	10 °C

Table 4
Parameters for the 1000 MW sCO_2 coal-fired power plant concept design [23,35,39,52].

Parameters	Values
Cycle type	Indirect
boiler type	Pulverized coal boiler
Net power (W_{net})	1000 MWe
Inlet temperature of compressor C1 and C1′ ($T_{1'}$, T_1)	32 °C
Inlet pressure of compressor C1′ (P_1)	7.6 MPa
Inlet temperature of turbine T1, T2 and T3 (T_6, $T_{6'}$ and $T_{6''}$)	630 °C
Inlet pressure of turbine T1 (P_1)	35 MPa
Isentropic efficiency of turbine T1 ($\eta_{T1,s}$)	91.58%
Isentropic efficiency of turbine T2 ($\eta_{T2,s}$)	91.86%
Isentropic efficiency of turbine T3 ($\eta_{T3,s}$)	92.39%
Isentropic efficiency of compressors ($\eta_{C,s}$)	89%
Pressure drop in regenerators (ΔP)	0.1 MPa
Pinch temperature difference in LTR and MTR (ΔT)	8 °C
Primary air temperature entering air preheater	31 °C
Primary air temperature leaving air preheater	320 °C
Ratio of primary air flow rate to the total air flow rate	19%
Secondary air temperature entering air preheater	23 °C
Ratio of secondary air flow rate to the total air flow rate	81%
Environment temperature (T_0)	20 °C
Excess air coefficient (α)	1.2
Ratio of low temperature flue gas recirculation (x_{rec})	27%
Pinch temperature difference between flue gas and CO_2 at point 5b (ΔT_{5b})	40 °C
Pinch temperature difference between flue gas and CO_2 at point 4b (ΔT_{4b})	20 °C

Table 6. The system adopted TC + DRH + IC cycle configuration which is recommended by general cycle analysis in section 2. TC is presented by LTR, MTR, C2 and C3, IC is presented by cooler 2 arranged between C1′ and C1, DRH is presented by T1, T2, T3 and heater modules between three turbines. Besides, overlap energy utilization is utilized to absorb the flue gas energy over the whole temperature range, which is presented by heater4a, heater4b, AP1, AP2 and EAP. The proposed cycle also integrates the module boiler design to suppress the pressure drop penalty effect, heaters 1–3 are subdivided into ten modules. Pressure drops of three heaters are 0.6 MPa, 0.3 MPa and 0.14 MPa, respectively, which is even smaller than supercritical water-steam boiler [49]. The flue gas recirculation is used to keep the heater surface temperature in an accepted level, here, recirculating part of flue gas with the ratio of 27% at the inlet position of the AP1 and sending it to the furnace. The total air flow rate after leaving AP1 is decoupled into two streams. The primary stream, accounting for 19%, directly returns to the furnace for combustion. The secondary stream, accounting for 81%, is continued to be heated by a portion of CO_2 in EAP and a portion of moderate flue gas energy in AP2 consecutively and finally returns to furnace for combustion. AP2 and heater 4a'' are arranged in parallel to further extract moderate/low temperature flue gas energy. At the main vapor parameters of 630 °C/35 MPa, the thermal efficiency η_{th} is up to 54.43%. As the formula (34), Power efficiency η_e is the product of thermal efficiency η_{th}, boiler efficiency η_b and pipeline efficiency η_p, where η_{boiler} is 94.71% calculated by anti-method and η_p is a setting value to be 99% [24]. Finally, η_e is 51.03%, which is larger than 48.12% of the advanced supercritical water-steam power plant [5]. Such efficiency improvement

Table 5
Energy and exergy equations for compressors, turbines and heat exchangers of sCO_2 cycle [39,44].

Components	Energy and exergy equations
1, C1', 2'	$\eta_{C,s} = \frac{h_{2's}-h_1}{h_{2'}-h_1}, w_{C1'} = (1-x_{C2}-x_{C3})(h_{2'}-h_1);$ $i_{C1'} = w_{C1'} - (1-x_{C2}-x_{C3})(e_{2'}-e_1)$
1', C1, 2	$\eta_{C,s} = \frac{h_{2s}-h_{1'}}{h_2-h_{1'}}, w_{C1} = (1-x_{C2}-x_{C3})(h_2-h_{1'});$ $i_{C1} = w_{C1} - (1-x_{C2}-x_{C3})(e_2-e_{1'})$
10, C2, 3	$\eta_{C,s} = \frac{h_{10s}-h_3}{h_{10}-h_3}, w_{C2} = x_{C2}(h_{10}-h_3), i_{C2} = w_{C2} - x_{C2}(e_{10}-e_3)$
9, C3, 4	$\eta_{C,s} = \frac{h_{9s}-h_4}{h_9-h_4}, w_{C3} = x_{C3}(h_9-h_4), i_{C3} = w_{C3} - x_{C3}(e_9-e_4)$
5, T1, 6	$\eta_{T1,s} = \frac{h_5-h_6}{h_5-h_{6s}}, w_{T1} = h_5-h_6; i_{T1} = e_5-e_6-w_{T1}$
5', T2, 6'	$P_{6'} = \sqrt[3]{P_5^2P_7}, \eta_{T2,s} = \frac{h_{5'}-h_{6'}}{h_{5'}-h_{6's}}, w_{T2} = h_{5'}-h_{6'}; i_{T2} =$ $e_{5'}-e_{6'}-w_{T2}$
5'', T3, 6''	$P_{6''} = \sqrt[3]{P_5P_7^2}, \eta_{T3,s} = \frac{h_{5''}-h_{6''}}{h_{5''}-h_{6''s}}, w_{T3} = h_{5''}-h_{6''}; i_{T3} =$ $e_{5''}-e_{6''}-w_{T3}$
2, 3, 10, 9, LTR	$T_{10} = T_2 + \Delta T_{LTR}, (1-x_{C2}-x_{C3})(h_3-h_2) =$ $(1-x_{C3})(h_9-h_{10}); i_{LTR} =$ $(1-x_{C3})(e_9-e_{10}) - (1-x_{C2}-x_{C3})(e_3-e_2)$
3, 4, 9, 8, MTR	$T_9 = T_3 + \Delta T_{MTR}, x_{C3} = 1 - \frac{h_8-h_9}{h_4-h_3}; i_{MTR} =$ $(e_8-e_9) - (1-x_{C3})(e_4-e_3)$
4, 5, 8, 7, HTR	$T_8 = T_4 + \Delta T_{HTR}, (1-x_{EAP})(h_7-h_8) = (1-x_{Heater\,4})(h_5-h_4);$ $i_{HTR} = (1-x_{EAP})(e_7-e_8) - (1-x_{Heater\,4})(e_5-e_4)$
10, 1, Cooler	$i_{Cooler} = (1-x_{C2}-x_{C3})(e_{10}-e_1)$
2', 1', Intercooler	$P_{2'} = \sqrt{P_1P_2}, i_{Intercooler} = (1-x_{C2}-x_{C3})(e_{2'}-e_{1'})$

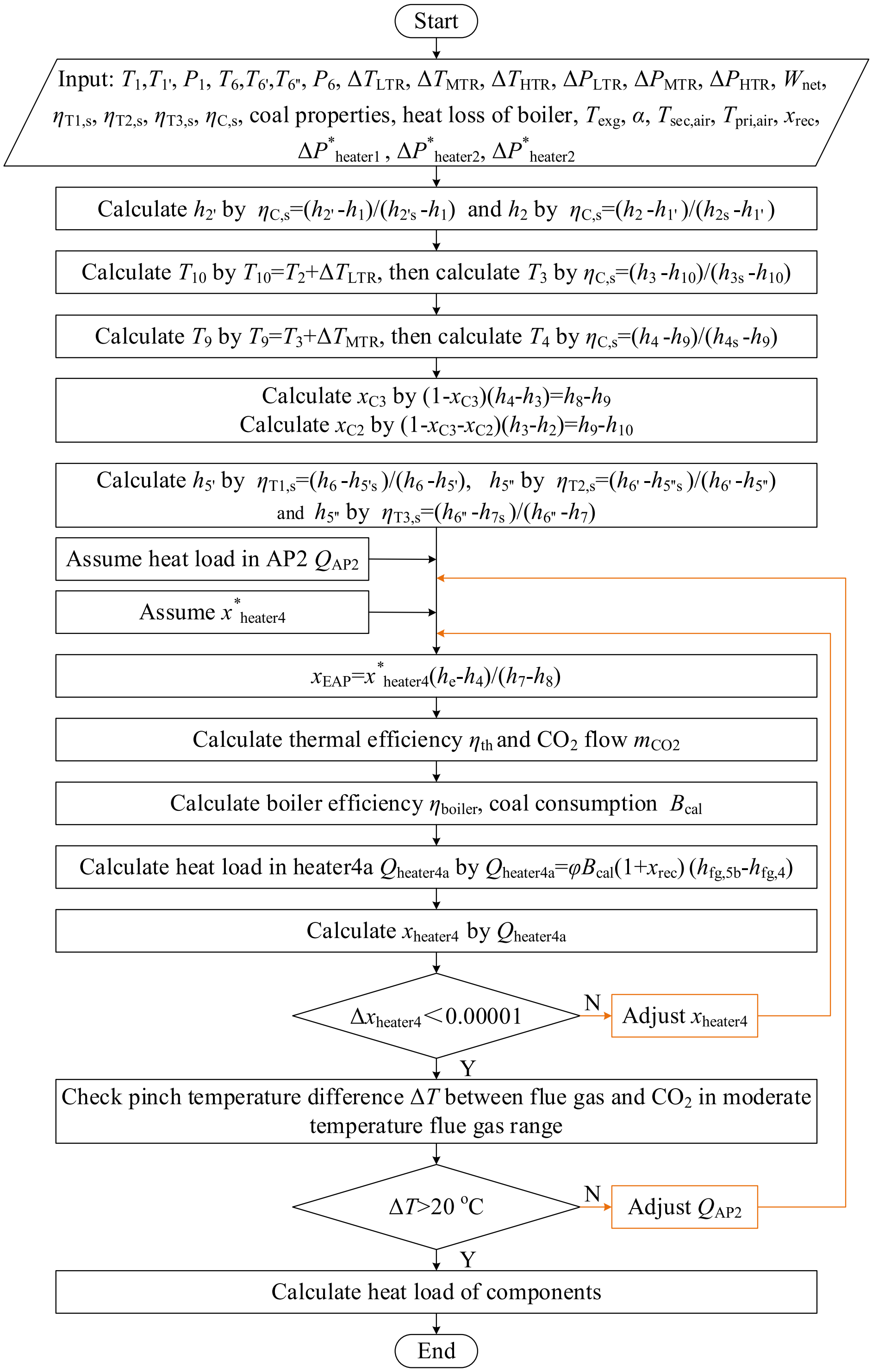

Fig. A1. Computation scheme of thermodynamic cycle.

Table 6
Properties of the designed coal [44].

C_{ar}	H_{ar}	O_{ar}	N_{ar}	S_{ar}	A_{ar}	M_{ar}	V_{daf}	Q_{LHV}
61.70	3.67	8.56	1.12	0.60	8.80	15.55	34.73	23,442

C (carbon), H (hydrogen), O (oxygen), N (nitrogen), S (sulfur), A (ash), M (moisture), V (volatile).Subscripts ar, d, af mean as received, dry and ash free, $C_{ar} + H_{ar} + O_{ar} + N_{ar} + S_{ar} + A_{ar} + M_{ar} = 100$.

Table 7
Components of boiler heat loss.

q_4	q_3	q_2	q_5	q_6	η_{boiler}
0.3	0	4.44	0.5	0.05	94.71

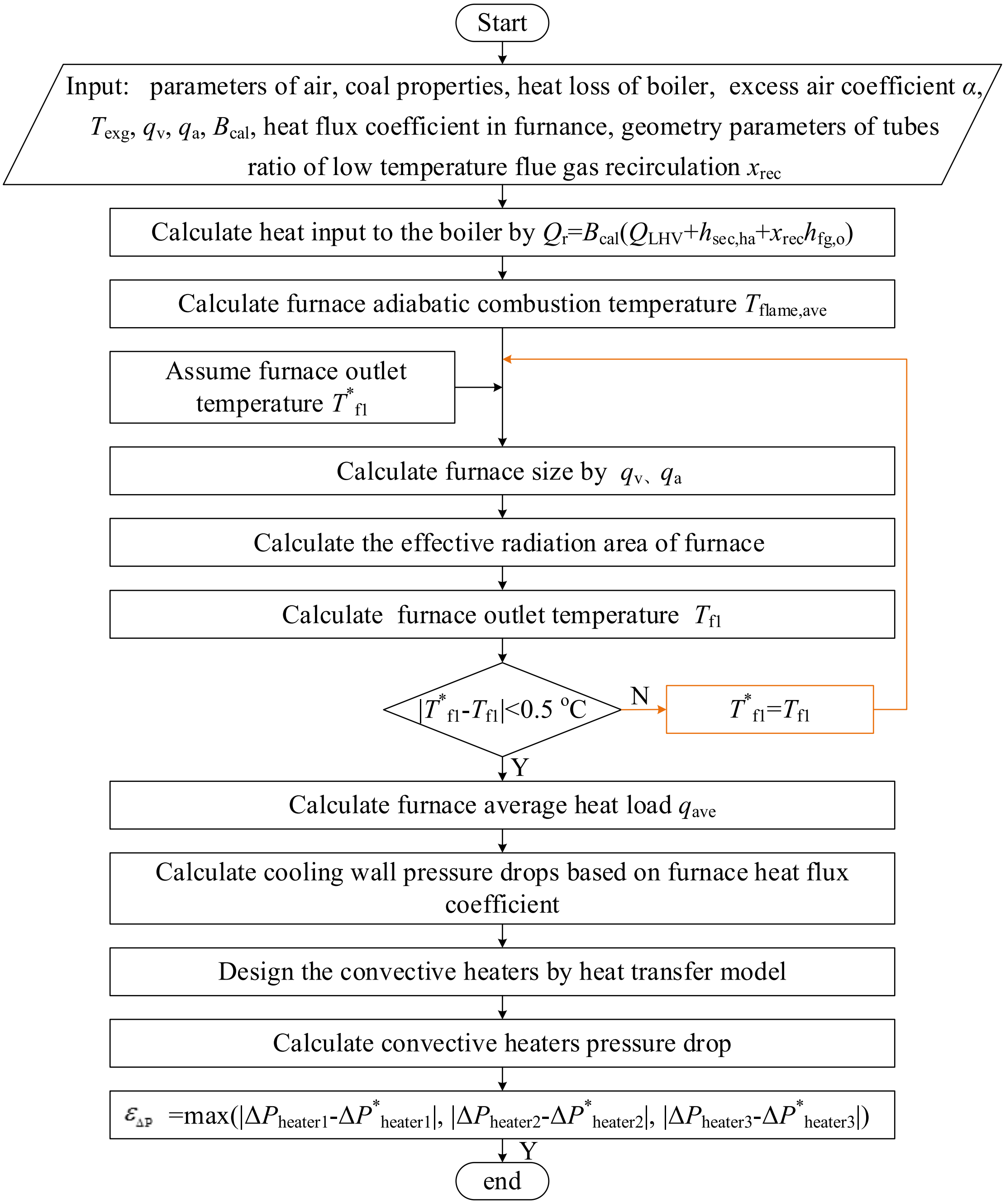

Fig. A2. Computation scheme of boiler design and thermal–hydraulic characteristics.

Table 8
Economic model of components [50].

Components	Economic model	Installation Cost Percentage (%)	
		Material	labor
Boiler	$C_{boiler} = 820800Q^{0.7327} \times f_{boiler}\ f_{boiler} = \begin{cases} 1\ ,\ T_{max} < 550^oC \\ 1 + 5.4 \times 10^{-5}(T_{max} - 550^oC)^2, T_{max} \geqslant 550^oC \end{cases}$	50	
Recuperators	$C_{recup} = 49.45UA^{0.7544} \times f_{recup}\ f_{recup} = \begin{cases} 1\ ,\ T_{max} < 550^oC \\ 1 + 0.02141(T_{max} - 550^oC)^2, T_{max} \geqslant 550^oC \end{cases}$	2	3
Coolers	$C_{cooler} = 32.88UA^{0.75}$	8	12
Turbines	$C_{tur} = 182600W_{tur}^{0.5561} \times f_{tur}\ f_{tur} = \begin{cases} 1\ ,\ T_{max} < 550^oC \\ 1 + 1.106 \times 10^{-4}(T_{max} - 550^oC)^2, T_{max} \geqslant 550^oC \end{cases}$	8	12
Compressors	$C_{com} = 1230000W_{com}^{0.3992}$	8	12
Generators	$C_{gen} = 108900W_e^{0.5463}$	8	12

Table 9
Assumed values for economic analysis.

Parameter	values
O&M operations OM ($/kWe)	30.00
O&M escalation rate er (%)	3.00
Plant lifetime NY (years)	30.00
Plant utilization factor u (%)	0.85
Discount rate r (%)	12.00
coal price c_{coal} ($/t)	119.56

saves 175.2 kilotons of coal and reduces 396.4 kilotons of CO_2 emission for 1000 MW capacity in a fascial year.

$$\eta_e = \eta_{th}\eta_{boiler}\eta_p \tag{34}$$

Fig. 11 shows cascade utilization of flue gas energy. The flue gas energy is divided into high, moderate and low temperature regions, with thermal loads 1718.6 MW, 219.4 MW and 302.3 MW, respectively. 1783.3 °C represents the flame temperature, 603.1 °C and 435.0 °C are called interface temperatures among the three regions. Two overlap energy utilization zones are marked with bright color, with temperature range 662.7 ~ 603.1 °C and 603.1 ~ 513.0 °C, correspondingly thermal loads 81.1 MW and 118.8 MW. The exhaust flue gas temperature is as low as 120.0 °C.

4.2. Energy balances of the sCO_2 power plant

As shown in Fig. 12, Sankey diagram is used to visualize energy flows, energy balances and energy losses of the sCO_2 coal-fired power plant. The widths of the blocks and lines represent the amount of energy and the length doesn't have physical meaning. Taking boiler as an example, the input energy contains three parts, chemical energy of the fuel, extra heat of bottom cycle carried by air, heat carried by sCO_2 after absorbing the regenerative energy, respectively. The output energy enters the turbines except a few energy loss caused by exhaust flue gas. For turbine, input energy from boiler is converted to shaft work of turbines at first, and the rest is divided into two parts, most of which enter HTR and a small part into EAP. For recuperators, energy transfer and conversion take place inside the system, without work done, work consumed and energy loss. Fig. 13 shows the thermal load distribution of various components for the system. The power plants are divided into two parts: the boiler system and the power cycle. For 1000 MWe net power output, compressors consume 555 MW compression work. Thermal load of recuperators account for 3741 MW, which is 3.7 times of the net power output, indicating that sCO_2 cycle is a highly heat recovery system. Regarding the system as a whole, input energy, energy loss and output energy across the whole sCO_2 cycle system are listed in Table 10. Chemical energy of the fuel is 1959.7 MW, as the only input energy. Electric power output is 1000 MW as the only output energy, accounting for 51.03%, which is the power generation efficiency of the system. Energy losses in boiler, coolers and pipeline are 103.7 MW, 837.3 MW and 18.6 MW, respectively, among which the highest energy loss occurs in coolers, accounting for 42.73%.

Table 10
Input energy, energy loss and output energy across the whole sCO_2 cycle system.

Items	Energy/MW	Ratio/%
Input energy		
Fuel	1959.7	1
Energy loss		
Boiler	103.7	5.29%
Coolers	837.3	42.73%
Pipe	18.6	0.95%
Output energy		
Electric power output	1000.0	51.03%
Energy efficiency	51.03%	

4.3. Exergy balances of the sCO_2 power plant

Exergy flows through the coal-fired sCO_2 power plant are marked in Sankey diagram shown in Fig. 14. Similar to Sankey diagram of energy, the widths of the blocks and lines represent the amount of exergy and the length don't have physical meaning. Input exergy, exergy loss and output exergy across the whole sCO_2 cycle system are listed in Table 11. The only exergy input of the power plants is 2008.1 MW from chemical energy of the fuel. The only exergy output is considered to be the work output of 1000 MW. Thus, the exergy efficiency of the power plants is 49.80%. Different from energy loss only existing in boiler, coolers and pipeline (see Fig. 12), exergy loss occurs in any component, totally 1008.15 MW. For the coolers, the exergy destruction is 57.48 MW, only accounting for 2.86% of total exergy inputs, far less than 42.73% of energy loss. The largest exergy destruction exists in the boiler, which account for approximately 40.50% of total exergy inputs and 80.68% of total exergy destruction and loss (see Fig. 15(a)). As shown in Fig. 15(b), the exergy loss in boiler contains four parts: (i) Combustion process, converting chemical energy into thermal energy, accounting for 56.47% of boiler exergy loss. (ii) Mixing process between the low temperature recirculation flue gas and high temperature combustion flame. (iii) Heat transfer process with temperature difference between flue gas and CO_2 in tubes. Fig. 16 shows the heat transfer process in the tail flue. (iv) Energy loss process due to exhaust gas and heat dissipation to environment.

4.4. Economic analysis of the sCO_2 power plant

Economy is an important aspect to enhance market competitiveness of the sCO_2 power plant besides plant efficiency, which will accelerate the commercialization of sCO_2 power cycles in general. Table 12 lists the equipment cost share percentage. For 1000 MW capacity, the total cost consumption of equipment is estimated to reach 1459.85 M$, combining with the labor and materials installation costs, which is higher than the traditional steam power plant. But over an entire 30 years lifetime of the power plant, the levelized cost of electricity (LCOE) is 36.58 $/MWh (see Table 13) for sCO_2 power system, which is lower than the water-steam system [52]. Besides, coal consumption of the sCO_2 power system for power supply b_g is 244.31 g/kWh with the reason that the electric generation efficiency η_e is higher to 51.03%.

Regenerator is recognized as key technology for the development of sCO_2 cycle [50]. The lower pinch temperature of regenerators is selected, the higher plant efficiency is and more expensive the plant is due to the increase of surface area and fabrication difficulty [50]. Among all the components cost estimation shown in Table 12, the proportion of regenerators is the largest, accounting for 48.47%. Besides, boiler accounts for about 29.25% of the power plant costs, coolers accounting for about 2.82%, turbines and compressors accounting for another 5.5%, and the other auxiliary equipment accounting for about 13.19%.

Table 11
Input exergy, exergy loss and output exergy across the whole sCO_2 cycle system.

Items	Energy/MW	Ratio/%
Input exergy		
Fuel	2008.1	1
Exergy destruction and loss		
Boiler	813.3	40.50%
Turbines	47.9	2.38%
Compressors	37.9	1.89%
Recuperators	51.5	2.57%
Coolers	57.5	2.86%
Output exergy		
Electric power output	1000.0	49.80%
Exergy efficiency	49.80%	

Table 12
Costs of various components of the sCO_2 coal-fired power plant.

Components		Cost/M$	Ratio/%
Boiler		29.25	29.25
Recuperators	HTR	49.82	48.87
	MTR	92.48	
	LTR	62.66	
Turbines	T1	12.34	2.93
	T2	11.95	
	T3	12.00	
Compressors	C1′	5.63	2.54
	C1	10.25	
	C2	12.15	
	C3	12.28	
Coolers	Cooler	28.28	2.82
	Intercooler	13.57	
Generators		5.69	0.40
Others		188.38	13.19
Total equipment investment		1459.85	1.00

Table 13
Overall performance data for the sCO_2 coal-fired power plant.

Parameter	values
Net power W_{net}(MW)	1000.00
Cycle thermal efficiency η_{th} (%)	54.43
Boiler efficiency η_b(%)	94.71
Electric generation efficiency η_e (%)	51.03
Coal consumption for power supply b_g(g/kWh)	244.31
Levelized cost of electricity LCOE($/MWh)	36.58

5. Conclusion

Following conclusions can be drawn based on the present study:

1) The roadmap to reach the efficiency limit for sCO_2 coal-fired power plant is proposed, reflected in two levels. The first level considers general analysis of sCO_2 cycle. By comparing the cycle performances of RC, TC, TC + RH, TC + DRH, and TC + DRH + IC, we conclude that TC + DRH + IC is applicable to reach the high system efficiency. The second level regards the sCO_2 cycle coupling with the boiler. It is concluded that OEU successfully absorbs flue gas energies over entire temperature range, and the partial flow mode is applicable to decrease pressure drops of boiler.
2) For comprehensive utilization of TC + DRH + IC, RH and TC contribute the first and second largest contribution to increase the system efficiency. IC and DRH make similar contribution for efficiency improvement. More stages compressions beyond 3 are not recommended, because the efficiency improvement is limited but increases the system complexity when the compressions stages are beyond three.
3) At the main vapor parameters of 35 MPa/630 °C, the proposed cycle attains the thermal efficiency of 54.43%. The electricity efficiency is 51.03%, which is higher than 48.12% for a supercritical water-steam power plant at the same capacity. Such efficiency improvement saves 175.2 kilotons of coal and reduces 396.4 kilotons of CO_2 emission in a fascial year.
4) For 1000 MWe net power output, compressors consume 555 MW compression work. Thermal load of recuperators account for 3741 MW, which is 3.7 times of the net power output, indicating that sCO_2 cycle is a highly heat recovery system.
5) For the proposed system, over an entire 30 years lifetime of the power plant, the levelized cost of electricity (LCOE) is 36.58 $/MWh, and the coal consumption for power supply b_g is 244.31 g/kWh. The LCOE and b_g are significantly lower than those of water-steam Rankine cycle power plant. This comparison indicates better economic feature of the sCO_2 power plant than water-steam power plant.

CRediT authorship contribution statement

Zhaofu Wang: Methodology, Software, Investigation, Writing – original draft. **Haonan Zheng:** Software, Investigation. **Jinliang Xu:** Conceptualization, Supervision, Funding acquisition, Writing – review & editing. **Mingjia Li:** Conceptualization, Methodology. **Enhui Sun:** Conceptualization, Methodology, Writing – review & editing. **Yuandong Guo:** Investigation. **Chao Liu:** Methodology, Validation. **Guanglin Liu:** Formal analysis.

Declaration of Competing Interest

The authors declare that they have no known competing financial interests or personal relationships that could have appeared to influence the work reported in this paper.

Data availability

Data will be made available on request.

Acknowledgements:

This work was supported by Natural Science Foundation of China (52130608, 51821004).

References:

[1] Wei Y, Chen K, Kang J, Chen W, Wang X, Zhang X. Policy and management of carbon peaking and carbon neutrality: a literature review. Engineering 2022.
[2] Xu G, Schwarz P, Yang H. Adjusting energy consumption structure to achieve China's CO_2 emissions peak. Renew Sustain Energy Rev 2020;122:109737.
[3] National Bureau of Statistics of China. China energy statistical yearbook. Beijing: China Statistics Press; 2020.
[4] Murakoshi T, Suzuki K, Nonaka I, Miura H. Microscopic analysis of the initiation of high-temperature damage of Ni-Based heat-resistant alloy. In ASME 2016 international Mechanical engineering congress and exposition, Phoenix, Arizona, USA.
[5] Fan H, Zhang Z, Dong J, Xu W. China's R&D of advanced ultra-supercritical coal-fired power generation for addressing climate change. Therm Sci Eng Prog 2018;5: 364–71.
[6] Xu J, Liu C, Sun E, Xie J, Li M, Yang Y, et al. Perspective of S-CO_2 power cycles. Energy 2019;186:115831.
[7] Sulzer G. Verfahren zur Erzeugung von Arbeit aus Warme. Swiss Patent 1950;599.
[8] Feher EG. The supercritical thermodynamic power cycle. Energy conversion 1968; 8(2):85–90.
[9] Angelino G. Carbon dioxide condensation cycles for power production. J Eng Power, ASME 1968;90(3):287–95.
[10] Dostal V. A supercritical carbon dioxide cycle for next-generation nuclear reactors. Department of Nuclear Engineering. USA: MIT; 2004.
[11] Gao C, Wu P, Shan J, Huang Y, Zhang J, Wang L. Preliminary study of system design and safety analysis methodology for supercritical carbon dioxide Brayton cycle direct-cooled reactor system. Ann Nucl Energy 2020;147:107734.
[12] Park JH, Yoon J, Eoh J, Kim H, Kim MH. Optimization and sensitivity analysis of the nitrogen Brayton cycle as a power conversion system for a sodium-cooled fast reactor. Nucl Eng Des 2018;340:325–34.
[13] Park JH, Park HS, Kwon JG, Kim TH, Kim MH. Optimization and thermodynamic analysis of supercritical CO_2 Brayton recompression cycle for various small modular reactors. Energy 2018;160:520–35.
[14] Wang K, He Y. Thermodynamic analysis and optimization of a molten salt solar power tower integrated with a recompression supercritical CO_2 Brayton cycle based on integrated modeling. Energ Convers Manage 2017;135:336–50.
[15] Singh R, Miller SA, Rowlands AS, Jacobs PA. Dynamic characteristics of a direct heated supercritical carbon-dioxide Brayton cycle in a solar thermal power plant. Energy 2013;50:194–204.
[16] Yang J, Yang Z, Duan Y. Off-design performance of a supercritical CO_2 Brayton cycle integrated with a solar power tower system. Energy 2020;201:117676.
[17] Linares JI, Montes MJ, Cantizano A, Sánchez C. A novel supercritical CO_2 recompression Brayton power cycle for power tower concentrating solar plants. Appl Energy 2020;263:114644.
[18] Ruiz-Casanova E, Rubio-Maya C, Pacheco-Ibarra JJ, Ambriz-Díaz VM, Romero CE, Wang X. Thermodynamic analysis and optimization of supercritical carbon dioxide Brayton cycles for use with low-grade geothermal heat sources. Energ Convers Manage 2020;216:112978.

[19] Li Bo, Wang S-S, Wang K, Song L. Comparative investigation on the supercritical carbon dioxide power cycle for waste heat recovery of gas turbine. Energ Convers Manage 2021;228:113670.
[20] Pan P, Yuan C, Sun Y, Yan X, Lu M, Bucknall R. Thermo-economic analysis and multi-objective optimization of S-CO_2 Brayton cycle waste heat recovery system for an ocean-going 9000 TEU container ship. Energ Convers Manage 2020;221:113077.
[21] Liese E, Albright J, Zitney SA. Startup, shutdown, and load-following simulations of a 10 MWe supercritical CO_2 recompression closed Brayton cycle. Appl Energ 2020;277:115628.
[22] Li H, Zhang Y, Yao M, Yang Y, Han W, Bai W. Design assessment of a 5 MW fossil fired supercritical CO_2 power cycle pilot loop. Energy 2019;174:792–804.
[23] Le Moullec Y. Conceptual study of a high efficiency coal-fired power plant with CO_2 capture using a supercritical CO_2 Brayton cycle. Energy 2013;49:32–46.
[24] Xu J, Sun E, Li M, Liu H, Zhu B. Key issues and solution strategies for supercritical carbon dioxide coal fired power plant. Energy 2018;157:227–46.
[25] Bai W, Zhang Y, Yang Y, Li H, Yao M. 300 MW boiler design study for coal-fired supercritical CO_2 Brayton cycle. Appl Therm Eng 2018;135:66–73.
[26] Moisseytsev A, Sienicki J J. Transient accident analysis of a supercritical carbon dioxide brayton cycle energy converter coupled to an autonomous lead-cooled fast reactor. In: International Conference on Nuclear Engineering, Miami, Florida, USA; July 17-20, 2006.
[27] Moisseytsev A, Sienicki JJ. Investigation of alternative layouts for the supercritical carbon dioxide Brayton cycle for a sodium-cooled fast reactor. Nucl Eng Des 2009;239(7):1362–71.
[28] Padilla RV, Too YCS, Benito R, Stein W. Effects of relative volume-ratios on dynamic performance of a direct-heated supercritical carbon-dioxide closed Brayton cycle in a solar-thermal power plant. Appl Energ 2015;148:348–65.
[29] Ehsan MM, Duniam S, Li J, Guan Z, Gurgenci H, Klimenko A. Effect of cooling system design on the performance of the recompression CO_2 cycle for concentrated solar power application. Energy 2019;180:480–94.
[30] Padilla RV, Too YCS, Benito R, Stein W. Exergetic analysis of supercritical CO_2 Brayton cycles integrated with solar central receivers. Appl Energ 2015;148:348–65.
[31] Linares JI, Montes MJ, Cantizano A, Sánchez C. A novel supercritical CO_2 recompression Brayton power cycle for power tower concentrating solar plants. Appl Energ 2020;263:114644.
[32] Zhang F, Zhu Y, Li C, Jiang P. Thermodynamic optimization of heat transfer process in thermal systems using CO_2 as the working fluid based on temperature glide matching. Energy 2018;151:376–86.
[33] Sun E, Xu J, Li M, Li H, Liu C, Xie J. Synergetics: The cooperative phenomenon in multi-compressions S-CO_2 power cycles. Energy Conversion and Manag X 2020;7:100042.
[34] Sun E, Xu J, Hu H, Li M, Miao Z, Yang Y, et al. Overlap energy utilization reaches maximum efficiency for S-CO_2 coal fired power plant: A new principle. Energ Convers Manage 2019;195:99–113.
[35] Mecheri M, Le Moullec Y. Supercritical CO_2 Brayton cycles for coal-fired power plants. Energy 2016;103:758–71.
[36] Zhang Y, Li H, Han W, Bai W, Yang Yu, Yao M, et al. Improved design of supercritical CO_2 Brayton cycle for coal-fired power plant. Energy 2018;155:1–14.
[37] Park S, Kim J, Yoon M, Rhim D, Yeom C. Thermodynamic and economic investigation of coal-fired power plant combined with various supercritical CO_2 Brayton power cycle. Appl Therm Eng 2018;130:611–23.
[38] Sun E, Xu J, Li M, Liu G, Zhu B. Connected-top-bottom-cycle to cascade utilize flue gas heat for supercritical carbon dioxide coal fired power plant. Energ Convers Manage 2018;172:138–54.
[39] Liu C, Xu J, Li M, Wang Z, Xu Z, Xie J. Scale law of sCO_2 coal fired power plants regarding system performance dependent on power capacities. Energ Convers Manage 2020;226:113505.
[40] Zhu B, Xu J, Wu X, Xie J, Li M. Supercritical, “boiling” number, a new parameter to distinguish two regimes of carbon dioxide heat transfer in tubes. Int J Therm Sci 2019;136:254–66.
[41] Zhou J, Zhu M, Xu K, Su S, Tang Y, Hu S, et al. Key issues and innovative double-tangential circular boiler configurations for the 1000 MW coal-fired supercritical carbon dioxide power plant. Energy 2020;199:117474.
[42] Liu C, Xu J, Li M, Wang Q, Liu G. The comprehensive solution to decrease cooling wall temperatures of sCO_2 boiler for coal fired power plant. Energy 2022;252:124021.
[43] Yang D, Tang G, Fan Y, Li X, Wang S. Arrangement and three-dimensional analysis of cooling wall in 1000 MW S-CO_2 coal-fired boiler. Energy 2020;197:117168.
[44] Wang Z, Sun E, Xu J, Liu C, Liu G. Effect of flue gas cooler and overlap energy utilization on supercritical carbon dioxide coal fired power plant. Energ Convers Manage 2021;249:114866.
[45] Fan Q. Boiler principle. Beijing: China Electric Power Press; 2014 [in Chinese].
[46] Wang Z, Sun B, Wang J, Hou L. Experimental study on the friction coefficient of supercritical carbon dioxide in pipes. Int J Greenhouse Gas Conf 2014;25:151–61.
[47] Yang S, Tao W. Heat transfer. Beijing: Higher Education Press; 2006 [in Chinese].
[48] Yu C, Xu J, Sun Y. Transcritical pressure Organic Rankine Cycle (ORC) analysis based on the integrated-average temperature difference in evaporators. Appl Therm Eng 2015;88:2–13.
[49] Boilers-Theory CD. Design and operation. Xi’an: Xi’an Jiaotong University Press; 2008.
[50] Weiland N T, Lance W B, Pidaparti S. SCO_2 power cycle component cost correlations from doe data spanning multiple scales and applications. In: ASME, editor. Proceedings of ASME Turbo Expo 2019: Turbomachinery Technical Conference and Exposition, Phoenix, Arizona, USA; June 17-21, 2019.
[51] Calculating method of economical and technical index for thermal power plant. National Energy Administration; 2015.
[52] Xu J, Wang X, Sun E, Li M. Economic comparison between sCO_2 power cycle and water-steam Rankine cycle for coal-fired power generation system. Energ Convers Manage 2021;238:114150.
[53] Marchionni M, Bianchi G, Tassou SA. Techno-economic assessment of Joule-Brayton cycle architectures for heat to power conversion from high-grade heat sources using CO_2 in the supercritical state. Energy 2018;148:1140–52.